

Paleomagnetic determination of emplacement temperatures of pyroclastic deposits: an under-utilized tool

Greig A. Paterson · Andrew P. Roberts ·
Conall Mac Niocaill · Adrian R. Muxworthy ·
Lucia Gurioli · José G. Viramonté · Carlos Navarro ·
Shoshana Weider

Received: 30 January 2009 / Accepted: 29 October 2009 / Published online: 19 November 2009
© Springer-Verlag 2009

Abstract Paleomagnetic data from lithic clasts collected from Mt. St. Helens, USA, Volcán Láscar, Chile, Volcán de Colima, Mexico and Vesuvius, Italy have

been used to determine the emplacement temperature of pyroclastic deposits at these localities and to highlight the usefulness of the paleomagnetic method for determining emplacement temperatures. At Mt. St. Helens, the temperature of the deposits (T_{dep}) at three sites from the June 12, 1980 eruption was found to be $\geq 532^{\circ}\text{C}$, $\geq 509^{\circ}\text{C}$, and $510\text{--}570^{\circ}\text{C}$, respectively. One site emplaced on July 22, 1980 was emplaced at $\geq 577^{\circ}\text{C}$. These new paleomagnetic temperatures are in good agreement with previously published direct temperature measurements and paleomagnetic estimates. Lithic clasts from pyroclastic deposits from the 1993 eruption of Láscar were fully remagnetized above the respective Curie temperatures, which yielded a minimum T_{dep} of 397°C . Samples were also collected from deposits thought to be pyroclastics from the 1913, 2004 and 2005 eruptions of Colima. At Colima, the sampled clasts were emplaced cold. This is consistent with the sampled clasts being from lahar deposits, which are common in the area, and illustrates the usefulness of the paleomagnetic method for distinguishing different types of deposit. T_{dep} of the lower section of the lithic rich pyroclastic flow (LRPF) from the 472 A.D. deposits of Vesuvius was $\sim 280\text{--}340^{\circ}\text{C}$. This is in agreement with other, recently published paleomagnetic measurements. In contrast, the upper section of the LRPF was emplaced at higher temperatures, with $T_{dep} \sim 520^{\circ}\text{C}$. This temperature difference is inferred to be the result of different sources of lithic clasts between the upper and lower sections, with the upper section containing a greater proportion of vent-derived material that was initially hot. Our studies of four historical pyroclastic deposits demonstrates the usefulness of paleomagnetism for emplacement temperature estimation.

Electronic supplementary material The online version of this article (doi:10.1007/s00445-009-0324-4) contains supplementary material, which is available to authorized users.

Editorial responsibility: M. Ripepe

G. A. Paterson (✉) · A. P. Roberts
National Oceanography Centre, University of Southampton,
European Way, Southampton SO14 3ZH, UK
e-mail: greig.paterson@noc.soton.ac.uk

C. Mac Niocaill · S. Weider
Department of Earth Sciences, University of Oxford,
Oxford OX1 3PR, UK

A. R. Muxworthy
Department of Earth Science and Engineering,
Imperial College, London SW7 2AZ, UK

L. Gurioli
Department of Geology and Geophysics, SOEST,
University of Hawaii, 1680 East-West Road, Honolulu,
HI 96822, USA

J. G. Viramonté
Instituto Geonorte, Universidad Nacional de Salta,
Av. Bolivia 5150–4400, Salta, República Argentina

C. Navarro
Observatorio Vulcanológico, Universidad de Colima,
Av. Gonzalo de Sandoval 444, Colima, Colima
CP. 28045, Mexico

Keywords Emplacement temperature · Mt. St. Helens · Paleomagnetism · Pyroclastic deposits · Vesuvius · Volcán de Colima · Volcán Láscaar

Introduction

Pyroclastic density currents are one of the most deadly volcanic hazards (Tanguy et al. 1998; Witham 2005). Estimating emplacement temperatures for past pyroclastic eruptions helps to quantify risks in regional hazard assessments. The paleomagnetic approach to estimating emplacement temperatures was first suggested by Aramaki and Akimoto (1957), and has been applied occasionally during the succeeding decades (e.g., Mullineaux and Crandell 1962; Chadwick 1971; Wright 1978). Modifications introduced by Hoblitt and Kellogg (1979), and Kent et al. (1981) led to the method that is used today (McClelland and Druitt 1989; Clement et al. 1993; Bardot 2000; Cioni et al. 2004; McClelland et al. 2004; Porreca et al. 2007; Zanella et al. 2007). The paleomagnetic approach is as follows. During a pyroclastic eruption, explosive fragmentation of juvenile magma breaks up some of the existing volcanic structure and creates a deposit containing fragments of juvenile material and accidental lithic clasts. The accidental lithic clasts will have originally been magnetized prior to the eruption. If a pyroclastic density current was emplaced above ambient temperature, the clasts will have been heated during their incorporation into the deposit and will have then cooled in place after deposition. This heating and cooling will partially or completely reset the magnetization of the clasts. The portion of the magnetization that was reset during the eruption will be aligned with the ambient Earth's magnetic field. This produces two components of magnetization: the original, higher temperature component, which will be randomly oriented for an assemblage of clasts, and a lower temperature component that will consistently align with the Earth's magnetic field at the time of emplacement. Progressive thermal demagnetization can be used to isolate these two magnetization components. The highest temperature at which the low-temperature component is still present provides an estimate of the emplacement temperature of the clast.

Paleomagnetic determination of emplacement temperature

The approach outlined above yields the emplacement temperature of each individual clast. It may not repre-

sent the temperature reached by the deposit as a whole and it does not take into account the thermal history of the clasts. Clasts that were either cold or hot, prior to eruption, can be incorporated into a single deposit. Clasts that were cold will be initially heated in the deposit, and clasts that were originally hot will cool. There is a temperature at which the deposit will start to cool as a whole; this is identified by the lowest emplacement temperature of the sampled clasts. This temperature is defined as the equilibrium temperature by Bardot and McClelland (2000). Cioni et al. (2004) defined the deposit temperature (T_{dep}) slightly differently. They noted that thin pyroclastic deposits, or clasts that are near the boundaries of the deposit, may experience adverse cooling conditions and that the equilibrium temperature of Bardot and McClelland (2000) may not represent the true temperature of the deposit. Instead, they proposed a temperature estimate based on the overlap of the emplacement temperature of each clast at one locality. They exclude outliers of this overlapping range on the basis of adverse cooling or heating prior to deposition (Cioni et al. 2004; Zanella et al. 2007, 2008). In the case of a thin deposit, the approach of Bardot and McClelland (2000) should underestimate the true temperature of the deposit. Where the sampled deposits are a thermally closed system (i.e., the middle of a thick deposit) both approaches should yield similar results. We use the definition of T_{dep} from Bardot and McClelland (2000) (i.e., the lowest emplacement temperature) to demonstrate the usefulness of paleomagnetism for estimating emplacement temperatures of pyroclastic deposits.

Despite a large published literature on pyroclastics, relatively little work has concentrated on the temperatures of pyroclastic eruptions, with fewer still using paleomagnetism. Paleomagnetism has been used to determine the emplacement temperature of pyroclastic deposits in 39 published papers (Table 1). The original method proposed by Aramaki and Akimoto (1957) simply involved measurement of the natural remanent magnetization (NRM) of samples without demagnetization. If the NRM direction was consistent with the geomagnetic field at the time of the eruption, the clast was interpreted to have been emplaced hot; if not, then the clast was emplaced cold. Since then the paleomagnetic method of determining emplacement temperatures has been refined to include improved experimental techniques and data analysis. Hoblitt and Kellogg (1979) presented the first paleomagnetic emplacement temperature study to use progressive thermal demagnetization, and Kent et al. (1981) used orthogonal vector component plots (Zijderveld 1967) to separate the recorded paleomagnetic components.

Table 1 Previous studies using paleomagnetism to determine pyroclastic emplacement temperatures

	Authors	Location	Year
1.	Aramaki and Akimoto	Asama Bandai-san, Ko-Fuji	1957
2.	Mullineaux and Crandell	Mt. St. Helens	1962
3.	Chadwick	Gallatin Mountains	1971
4.	Crandell	Mt. St. Helens	1971
5.	Crandell and Mullineaux	Mt. St. Helens	1973
6.	Yamazaki et al.	Donzurubo	1973
7.	Wright	Santorini	1978
8.	Hoblitt and Kellogg	Mt. St. Helens	1979
9.	Kent et al.	Vesuvius	1981
10.	Zlotnicki et al.	Guadeloupe	1984
11.	McClelland and Druitt	Santorini	1989
12.	Downey and Tarling	Santorini	1991
13.	Tamura et al.	Shirahama Group	1991
14.	Clement et al.	Colima	1993
15.	McClelland and Thomas	Santorini	1993
16.	Pares et al.	Catalan Volc. Zone	1993
17.	Mandeville et al.	Krakatau	1994
18.	Bardot et al.	Santorini	1996
19.	De Gennaro et al.	Campi Flegrei	1996
20.	Moore et al.	Jemez Mountains	1997
21.	Grubensky et al.	Oregon Cascades	1998
22.	Smith et al.	Mt. Ruapehu	1999
23.	Bardot	Santorini	2000
24.	Bardot and McClelland	Santorini	2000
25.	Sawada et al.	Mt. Sambe	2000
26.	Mastrolorenzo et al.	Vesuvius	2001
27.	Zanella et al.	Vulcano	2001
28.	McClelland and Erwin	Mt. Ruapehu	2003
29.	Saito et al.	Yufu	2003
30.	Cioni et al.	Vesuvius	2004
31.	McClelland et al.	Taupo	2004
32.	Tanaka et al.	Unzen	2004
33.	Alva-Valdivia et al.	San Gaspar	2005
34.	Porreca et al.	Stromboli	2006
35.	Porreca et al.	Colli Albani	2007
36.	Zanella et al.	Vesuvius	2007
37.	Zanella et al.	Vesuvius	2008
38.	Sulpizio et al.	El Chicón	2008
39.	Di Vito et al.	Vesuvius	2009

Including Kent et al. (1981), only 30 papers have been published using the full demagnetization method (excluding Zlotnicki et al. (1984) who used paleointensities to estimate emplacement temperatures). A number of these papers deal primarily with the magnetic properties of the pyroclastic deposits and only report the emplacement temperatures in passing. Only 19 different localities have been studied. One quarter of the publications are based on data from Santorini, and are primarily from the paleomagnetic group at the University of Oxford. Their work on the extensive deposits of Santorini and the work of the group based at the University of Torino, Italy, represent the only attempts to document the thermal evolution of a pyroclastic volcano and changing emplacement temperatures with

changing eruptive styles. Paleomagnetism is therefore an under-utilized tool in volcanology, despite recent efforts by a few groups to use and promote the method. Below, we outline some of the assumptions, potential problems, and advantages of the paleomagnetic method for determining emplacement temperatures with respect to other techniques. We then present results from four volcanoes to highlight the potential and range of applications of the paleomagnetic method.

Non-ideal behaviour

A key assumption behind the paleomagnetic method for estimating emplacement temperatures is that the magnetic remanence acquired at the time of

emplacement is a thermal remanent magnetization (TRM) (Bardot and McClelland 2000; McClelland et al. 2004). Formation of a chemical remanent magnetization (CRM) can affect the blocking temperature spectrum of a sample, and can obscure the emplacement temperature as identified on orthogonal plots of paleomagnetic directions. McClelland et al. (2004) and Porreca et al. (2007) proposed the use of thermomagnetic curves or magnetic susceptibility-temperature curves to detect the possible presence of a CRM. If a Curie temperature of a clast coincides with its apparent emplacement temperature, then the magnetic remanence of the sample could be a CRM. Thermomagnetic measurements can be made rapidly and the most common magnetic mineral to acquire a CRM, maghemite, is readily identifiable on a thermomagnetic curve due to its inversion to hematite or magnetite during heating.

In addition to the possibility of CRM acquisition, the time-temperature dependence of magnetization (Néel 1949) means that if a clast is exposed to a magnetic field for a prolonged period of time, part of its magnetization will relax and align with the applied field. This is called a viscous remanent magnetization (VRM). The same VRM can be acquired if the clast is exposed to the same magnetic field for a shorter period of time, but at a higher temperature. This temperature dependence allows VRMs to be removed by thermal demagnetization in the laboratory. A VRM acquired by sampled clasts will record the geomagnetic field between the time of cooling and sample collection. For recent eruptions the VRM direction can be indistinguishable from the paleomagnetic direction acquired by clasts during emplacement. Therefore, the maximum temperature at which a VRM is removed in the laboratory provides a lower limit for emplacement temperature estimates. For a deposit of a given age, there is a minimum emplacement temperature that can be resolved using paleomagnetism. This is determined by the demagnetization temperature required to remove the VRM acquired during longest period of time that the deposit remains in a constant geomagnetic field. The age-temperature relation for VRM acquisition at ambient temperature (25°C) for common carriers of TRM is shown in Fig. 1.

For example, clasts containing single-domain (SD) magnetite from a 1 Ma deposit experienced the longest period of stable geomagnetic field during the Brunhes Chron (780 kyrs), therefore the minimum emplacement temperature that can be estimated is ~185°C, while for hematite this is ~290°C. Considering the Curie temperatures of these minerals (580°C and 675°C, respectively) gives a temperature range of ~400°C over which emplacement temperature estimates can be made. This extensive potential age range demonstrates the distinct

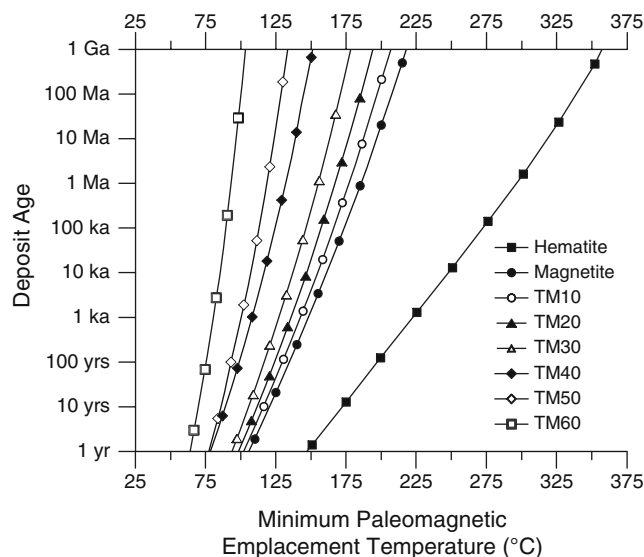


Fig. 1 Deposit age plotted versus minimum paleomagnetic emplacement temperature as predicted by viscous magnetization theory for hematite, magnetite and part of the titanomagnetite series (TM10–TM60). The curves are based on theory and the magnetite data of Pullaiah et al. (1975) and hematite data from Dunlop (1971). The titanomagnetite series curves are calculated from the Curie temperature scaling relationship suggested by Pullaiah et al. (1975) using data from Xu et al. (1996)

advantage of the paleomagnetic method over other approaches.

Another potential source of non-ideal behaviour arises from the presence of multidomain (MD) grains. When a magnetic grain grows large enough the magnetization no longer remains uniform as for SD grains and the magnetization is divided into regions (domains) of varying magnetization. Such grains have non-ideal paleomagnetic behaviour (e.g., Bol'shakov and Shcherbakova 1979; Shcherbakova et al. 2000; Fabian 2003), particularly with respect to paleointensity studies (e.g., Levi 1977). The remanence acquired by MD grains does not unblock at the same temperature at which it was blocked, which produces what is known as a partial TRM (pTRM) tail (i.e., a portion of magnetic remanence that demagnetizes above the acquisition temperature; Bol'shakov and Shcherbakova 1979). Such tails can commonly only be removed by demagnetization to the Curie temperature. The presence of a pTRM tail produces an overlap in the unblocking temperature spectra of different magnetization components in a sample, which will be evident as curvature on the vector component diagram. If only a single component of magnetization is present, the overlapping blocking temperatures will record the same direction, and the paleomagnetic directional analysis will be unaffected. The presence of MD grains will therefore not

compromise paleomagnetic emplacement temperature estimates.

Other methods for determining emplacement temperatures

Estimates of the emplacement temperature for a pyroclastic deposit can be made directly using a thermal probe or remotely, by satellite. Relatively few direct measurements have been published (e.g., Banks and Hoblitt 1981; Cole et al. 1998; Calder et al. 1999; Druitt et al. 2002), largely because of the risk associated with visiting an active volcanic region shortly after an eruption. Satellite observations using Advanced Very High Resolution Radiometer (AVHRR) imagery provide excellent spatial resolution, but are only capable of measuring temperatures up to $\sim 250^{\circ}\text{C}$ (Denniss et al. 1998).

Field evidence provides another means of studying the thermal history of a pyroclastic deposit. Features such as gas escape pipes, vesicles within the ash matrix, carbonized materials and discolouration of lithic fragments provide evidence of high temperature emplacement. However, these features are often not present or visible and do not always allow quantitative estimation of emplacement temperature. Other, more quantitative, methods have also been used. These include oxidation colours of pumice (Tsuboi and Tsuya 1930), infra-red spectroscopy of wood fragments (Maury 1971), and analysis of bone fragments (Capasso et al. 2000). Voight and Davis (2000) used the melting points of plastic bottles to estimate the emplacement temperatures of pyroclastic deposits at Merapi Volcano, Java, Indonesia. This novel approach has limited usefulness and only allows temperature estimates up to $\sim 150\text{--}250^{\circ}\text{C}$. Sawada et al. (2000) investigated use of the H/C ratio of carbonized wood as a paleo-thermometer. Controlled laboratory experiments and analysis were used to show that the correct heating temperature is recoverable with this method. When applied to Holocene pyroclastics, the H/C ratio method gave results that were consistent with paleomagnetic data (Sawada et al. 2000).

Sampling and experimental procedures

Several localities were studied here to demonstrate the widespread usefulness of the paleomagnetic method for determining emplacement temperatures of pyroclastic deposits. At all localities sampled in this study, ori-

ented hand specimens were collected using the method described by Tarling (1983). A horizontal line was marked, on a relatively flat surface, on each clast. The strike of this line and the dip of the surface were measured using a magnetic compass-clinometer. Cores with a diameter of 10 or 20-mm were then drilled from the clasts in the laboratory. Remanence measurements were made within a magnetically shielded laboratory using either a 2-G Enterprises cryogenic magnetometer, or a Molspin Minispin magnetometer at the University of Southampton or at the University of Oxford. Thermal demagnetization was carried out at $20\text{--}50^{\circ}\text{C}$ steps using either an ASC Scientific or a Magnetic Measurements thermal demagnetizer, both of which have residual fields of less than 50 nT. Following every heating step, the low-field magnetic susceptibility was measured at room temperature to check for signs of thermal alteration, using an Agico KLY-4S Kappabridge or a Bartington Instruments MS2B magnetic susceptibility meter. Additional sister samples were cut for rock magnetic measurements using a Princeton Measurements Corporation Vibrating Sample Magnetometer (VSM) at Southampton (maximum field of 1 T) and using an Agico KLY-2 Kappabridge magnetic susceptibility meter with furnace attachment at Oxford. Thermomagnetic curves were analysed using the RockMag Analyzer software (Leonhardt 2006), and susceptibility-temperature curves were analysed using the inverse susceptibility method outlined by Petrovský and Kapička (2006).

Results

Mt. St. Helens, USA

Mt. St. Helens is located in the Cascade Mountain Range of the western U.S.A., and is famous for its devastating eruption on May 18, 1980. This eruptive phase began in late March of 1980 with a series of generally short-lived eruptions. A magnitude 5.1 earthquake on May 18 triggered a landslide that caused rapid depressurization of the northern flank of the volcano, which triggered a lateral surge cloud. Activity continued at Mt. St. Helens during 1980 and the collapse of eruptive columns generated numerous pyroclastic density currents and deposits (Smithsonian Institution 1980). Within days to weeks of the pyroclastic deposits being emplaced, direct temperature measurements were taken by a group from the United States Geological Survey (Banks and Hoblitt 1981). The full procedure

and emplacement temperature analysis was presented by Banks and Hoblitt (1996). The debris avalanche was emplaced at low temperatures ($<100^{\circ}\text{C}$), while the lateral blast deposit was emplaced at slightly higher temperatures ($100\text{--}200^{\circ}\text{C}$). The pyroclastic deposits were much hotter, and were emplaced at 300°C to $>600^{\circ}\text{C}$ (Banks and Hoblitt 1996). Although the sites sampled in this study do not coincide exactly with those of Banks and Hoblitt (1996), the measured temperatures have been extrapolated based on the available data of Banks and Hoblitt (1996) and compared with our paleomagnetically determined temperatures.

A total of 113 clasts were collected from 6 different sites on the northern flank of Mt. St. Helens (Fig. 2). The lithic clasts include basalts, andesites and dacites. Thermal demagnetization up to around 125°C will remove potential viscous magnetizations, so low temperature steps are excluded from analysis of the recorded paleomagnetic directions. The measured samples have both single and multiple components of magnetic remanence (Fig. 3).

Sites MSH1 and 2 do not record a well-defined paleomagnetic direction (Fig. 4). Samples with two components of remanence indicate emplacement temperatures in the $330\text{--}390^{\circ}\text{C}$ temperature range. Direct measurements by Banks and Hoblitt (1996) give the temperature of the May 18 deposits in this area to be

$\sim 300\text{--}367^{\circ}\text{C}$. It seems most likely that the scattered paleomagnetic directions for these clasts therefore result from localized reworking and do not result from low temperature pyroclastic emplacement.

Sites MSH3, 5 and 6 all have well-defined paleomagnetic directions that record the expected geomagnetic field direction during 1980 (Fig. 4). Site MSH4 also records this direction, but it is poorly defined. However, the statistic $3R^2/N$, which provides a test for randomness (Rayleigh 1919), indicates that the paleomagnetic directions are statistically grouped at the 95% confidence level. The statistic will exceed 7.81 for a group of non-random paleomagnetic directions; the statistic at sites MSH3–6 exceeds 7.81. At both sites MSH1 and 2, $3R^2/N$ is ≤ 5.9 , which indicates that no consistent paleomagnetic direction is recorded.

Sixty-two samples from sites MSH3–6 have paleomagnetic directions that fall within 30° of the 1980 geomagnetic field direction. These samples were used to determine emplacement temperatures. The majority of samples have single components of magnetization, which means they were emplaced above the Curie temperature (T_c) of the constituent magnetic minerals. Curie temperatures of the clasts (Fig. 5a, b and Table 1, [Electronic supplementary material](#)) are $447\text{--}634^{\circ}\text{C}$ for the juvenile material, and $460\text{--}634^{\circ}\text{C}$ for the lithic clasts.

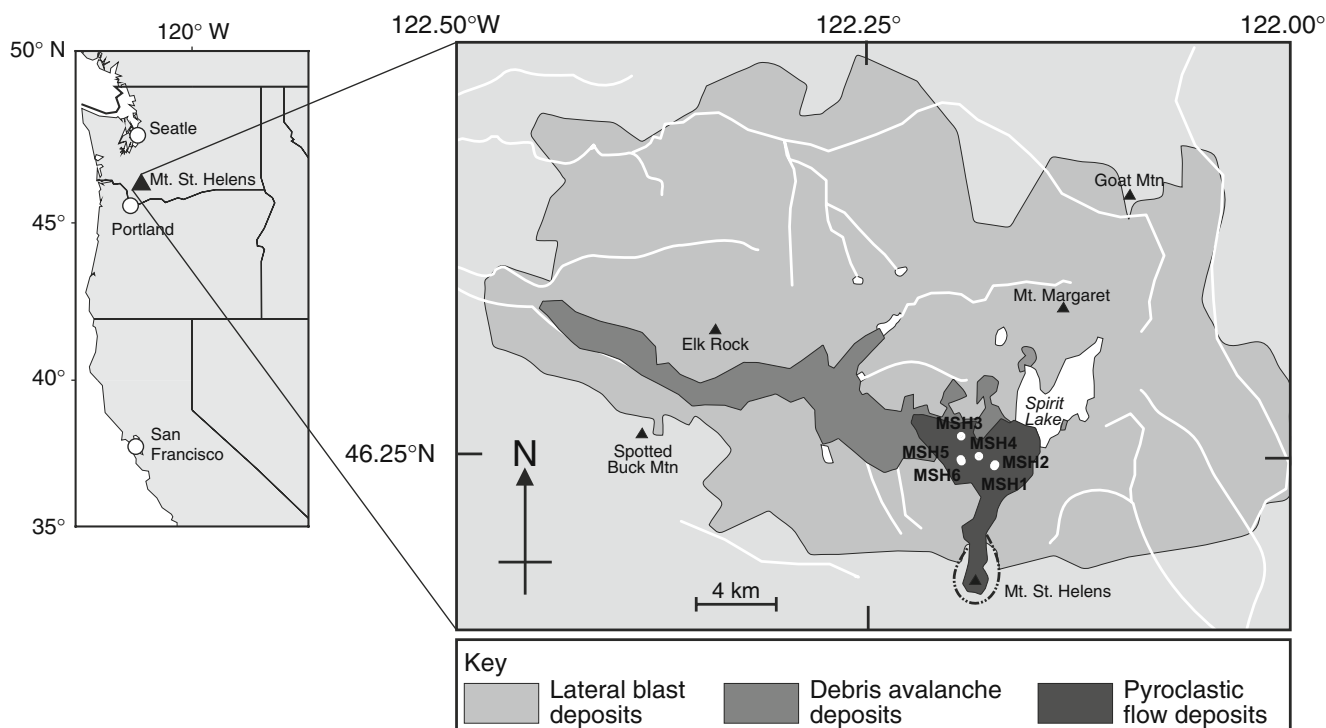
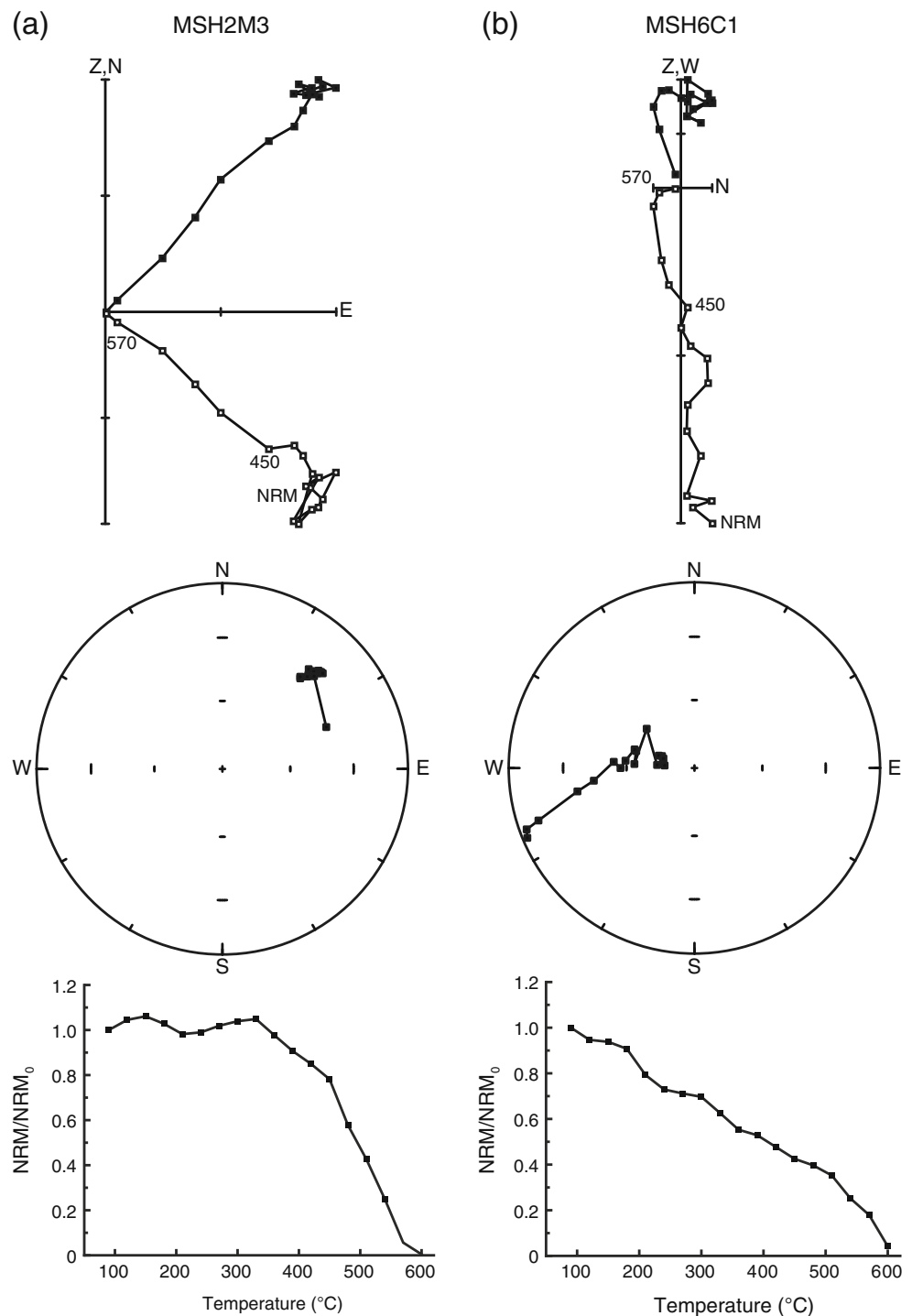


Fig. 2 Location and map of the pyroclastic deposits from the 1980 eruption of Mt. St. Helens, with the sampled localities indicated (MSH1–6). Modified after Erwin (2001)

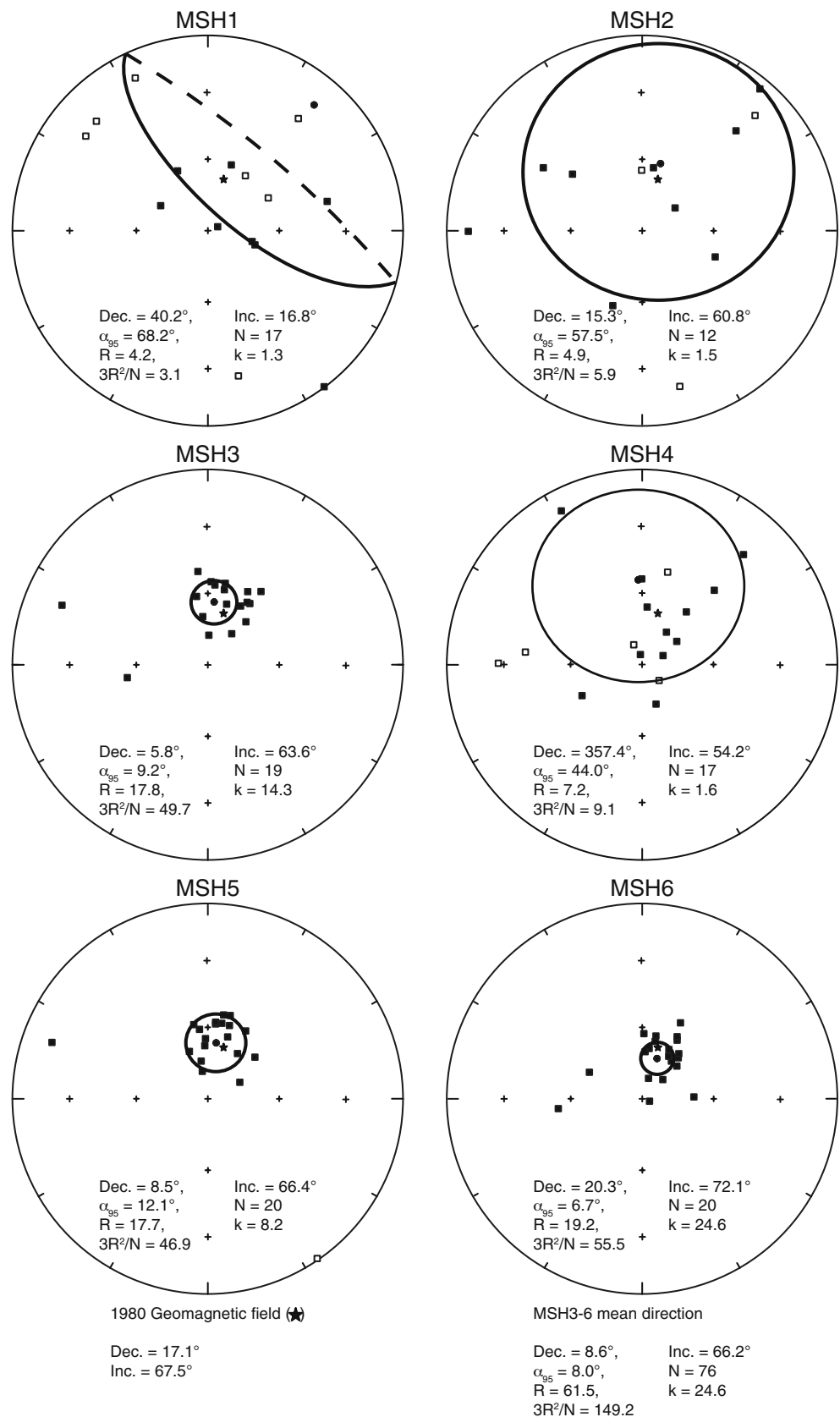
Fig. 3 Typical stepwise thermal demagnetization behaviour for the Mt. St. Helens samples. **a** Sample MSH2M3 has a single component of magnetization. In this case the clast has been reworked, so the direction does not align with the 1980 geomagnetic field direction. **b** Sample MSH6C1 has two components of magnetization. The intersection of the two components is not clearly defined and covers a temperature range of 510–570°C. In the vector component diagrams (*top*), *open symbols* denote projections onto the vertical plane, while *closed symbols* denote projections onto the horizontal plane. In the equal area stereographic projections (*middle*), *open symbols* denote upper hemisphere projections, while *closed symbols* denote lower hemisphere projections



Sites MSH3, 5 and 6 are all from the deposits emplaced on June 12, 1980. Extrapolation from the data of Banks and Hoblitt (1996) give emplacement temperatures at these three sites of around $540 \pm 30^\circ\text{C}$. At site MSH3, the June 12 deposits were rich in hot (≥ 447 – 595°C) juvenile material. The sampled lithic clasts were emplaced at or above T_c . T_{dep} can only be constrained to have been hotter than the lowest T_c ; for site MSH3

$T_{dep} \geq 532^\circ\text{C}$. This is in good agreement with the direct measurements of Banks and Hoblitt (1996) (Fig. 6). At site MSH5, where the juvenile content is lower, the lithic clasts also record only one paleomagnetic direction. The T_c of these clasts is 509 – 619°C . T_{dep} at MSH5 was $\geq 509^\circ\text{C}$. All but one sample at site MSH6 have single components of magnetization. The Curie temperatures of the lithic samples are 527 – 634°C . Sample

Fig. 4 Equal area stereographic projections of paleomagnetic directions recorded at each sample site at Mt. St. Helens. The **stars** denote the 1980 geomagnetic field direction. The *circles* represent the mean directions and *ellipses* are the α_{95} cones of confidence about the mean. *Open symbols* denote upper hemisphere projections, while *closed symbols* denote lower hemisphere projections. *Dec.* = declination; *Inc.* = inclination; α_{95} = semi-angle of 95% confidence; *N* = number of samples; *R* = the length of the mean vector; *k* = the estimate of the precision parameter, from Fisher (1953); and $3R^2/N$ = the statistic for randomness from Rayleigh (1919)



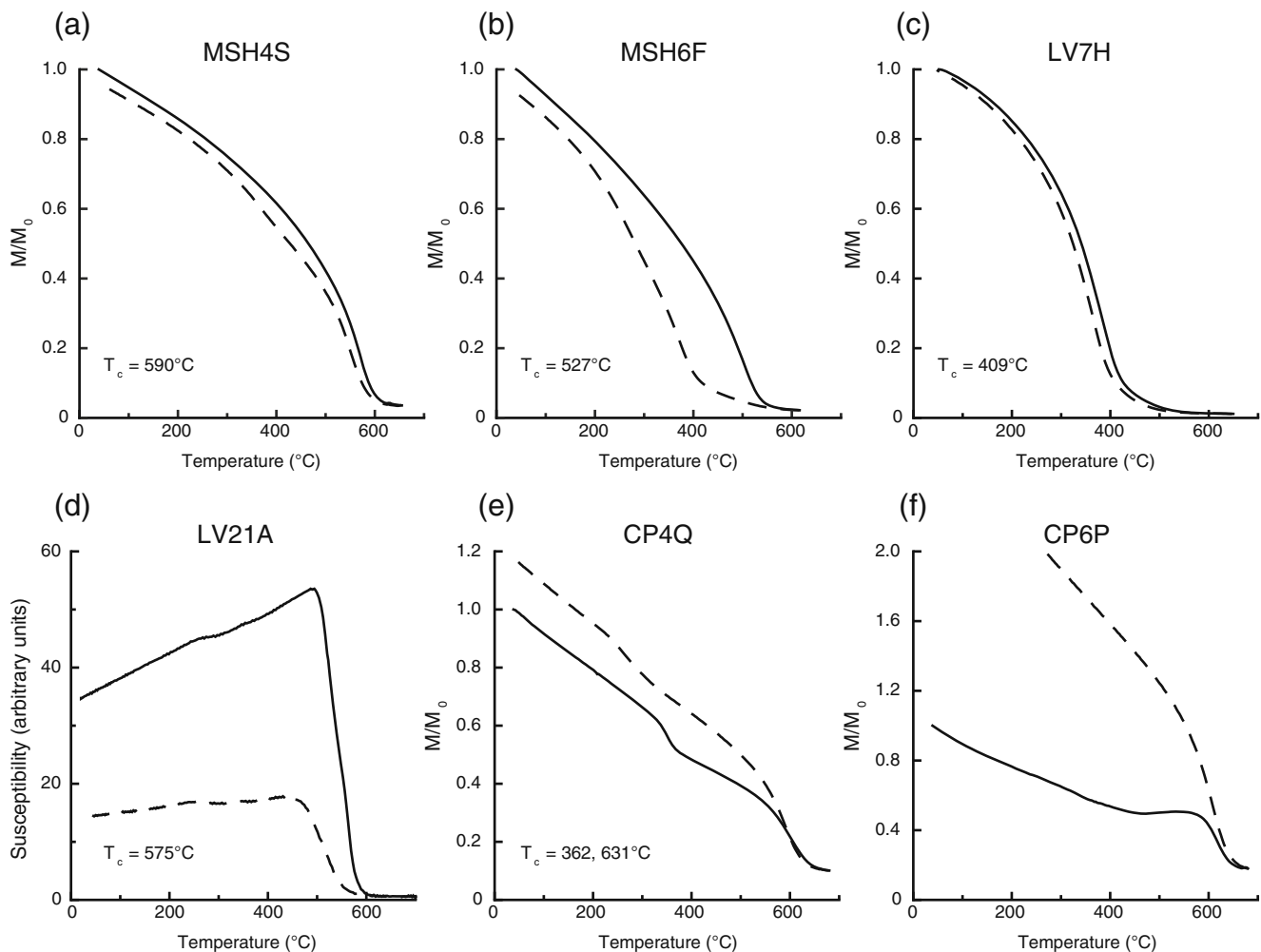


Fig. 5 Typical thermomagnetic and susceptibility-temperature curves for samples from **a, b** Mt. St. Helens, **c, d** Lásca, and **e, f** Vesuvius. *Solid (dashed) lines* represent the heating (cooling) cycle. **a** Clast MSH4S, which has a Curie temperature of 590°C. **b** Clast MSH6F, $T_c = 527^\circ\text{C}$. **c** Clast LV7H, $T_c = 409^\circ\text{C}$. **d** Susceptibility-temperature curve for clast LV21A, $T_c = 575^\circ\text{C}$. **e** Thermomagnetic curve for clast CP4Q, $T_c = 362, 631^\circ\text{C}$. The

coincidence of a Curie temperature with the emplacement temperature estimate may indicate that the remanence is of chemical and not thermal origin. **f** Thermomagnetic curve for clast CP6P, which is typical of maghemite inversion to hematite and magnetite. The remanence carried by this clast is therefore likely to be a CRM

MSH6C1 records two paleomagnetic directions. The intersection of these two directional components gives an emplacement temperature of 510–570°C. Although only one sample gives this result, it is considered to provide an accurate estimate of T_{dep} . We exclude the possibility of adverse cooling of this particular clast as it was sampled from a similar level within the deposit as clasts emplaced at temperatures above T_c , and so will have experienced the same cooling conditions. A paleomagnetic estimate of $T_{dep} = 510\text{--}570^\circ\text{C}$ is in excellent agreement with the measured value from Banks and Hoblitt (1996) of $540 \pm 30^\circ\text{C}$ (Fig. 6).

The deposit at site MSH4 was emplaced on July 22, 1980, and direct measurements by Banks and Hoblitt (1996) give an emplacement temperature of $>600^\circ\text{C}$.

The sampled clasts all have single components of magnetization. T_c for the lithic clasts range from 577 to 603°C, and for the juvenile material from 623 to 634°C. T_{dep} is taken to be $\geq 577^\circ\text{C}$. This estimate also agrees with the measurements of Banks and Hoblitt (1996) (Fig. 6).

Paleomagnetic emplacement temperatures of Erwin (2001) along with the new data presented here, and those of Sulpizio et al. (2008) from El Chichón, Mexico are plotted against available directly measured emplacement temperature data in Fig. 6. These data illustrate the accuracy of the paleomagnetic method for estimating emplacement temperatures of pyroclastic deposits and highlight the repeatability of paleomagnetic measurements.

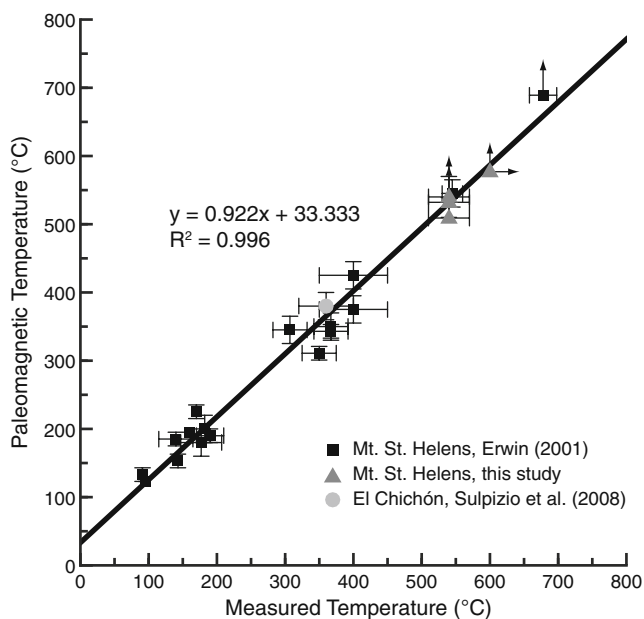


Fig. 6 Paleomagnetic emplacement temperature versus directly measured emplacement temperature for the 1980 pyroclastic deposits at Mt. St. Helens, USA (Erwin 2001, and this study), and El Chichón (Sulpizio et al. 2008). Both temperatures are strongly correlated, which indicates that the paleomagnetic approach is an accurate and viable method for determining the emplacement temperature of pyroclastic deposits. *Small error bars* have been removed for clarity; *arrows* indicate a minimum temperature estimate. The best-fit line was calculated using major-axis linear regression

Volcán Láscar, Chile

Láscar is a stratovolcano in the Chilean Andes, near the Argentinean border (Fig. 7a). On April 18, 1993, Láscar erupted for three days, in what was the largest historic eruption in the northern Andes (Smithsonian Institution 1993; Déruelle et al. 1995, 1996). Two intense eruptions on April 19 and 20 following the collapse of eruptive columns. The pyroclastic density currents resulted on April 19 and 20 following the collapse of eruptive columns. The pyroclastic deposits crop out on the volcano flanks up to 8.5 km from the summit toward the NW and SE (Fig. 7a) and cover an area of ~ 18.5 km².

The deposits contain a pumice-rich facies typically found in the frontal lobes and margins of the deposits and a lithic-rich facies in the interior of the deposits (Sparks et al. 1997). The pumice facies comprises an andesitic-dacitic juvenile component with a minor lithic content. The lithic-rich facies incorporates roughly equal proportions of eroded and vent-derived lithic clasts. These include fragments of the pre-existing

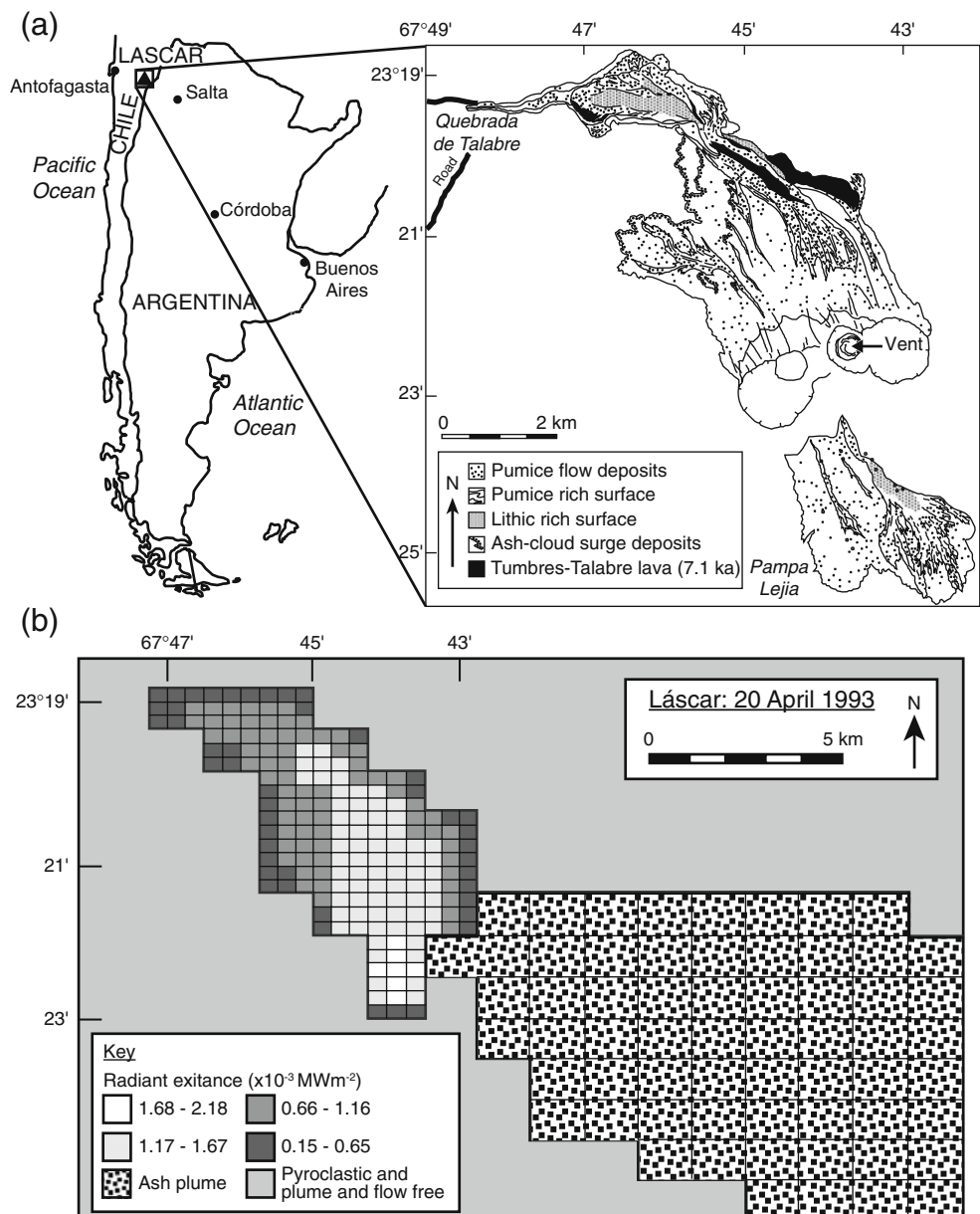
andesitic lava dome, formed in 1992, and clasts from the Tumbres-Talabre lava. Clasts of Tertiary ignimbrite and pink quartz rhyodacite were also incorporated, although they are not common (Déruelle et al. 1996; Sparks et al. 1997; Calder et al. 2000).

No direct temperature measurements of the pyroclastic deposits were made; however, due to its high altitude (5.5 km above sea level) and reduced cloud cover, Láscar is ideal for satellite observations (Oppenheimer et al. 1993; Wooster and Rothery 1997; Denniss et al. 1998; Wooster et al. 1998; Wooster 2001). Denniss et al. (1998), using AVHRR satellite imagery, produced a thermal radiance map of the 1993 Láscar pyroclastic deposits (Fig. 7b). Their results indicate a central hot area associated with the volcanic vent. The distinct shape of the northern deposits is also evident as areas with elevated temperatures. The southern slopes of Láscar were obscured by the ash plume, so no temperature estimates are available for these deposits. The available satellite data indicate that the minimum surface temperature of the deposits was ~ 185 – 265 °C. It must be noted this is the maximum temperature range that can be estimated using AVHRR imagery, so this range provides a minimum estimate of emplacement temperature for the pyroclastic density currents.

A total of 111 clasts, representing 31 sites from pyroclastic deposits on both flanks of Láscar, were collected. The sampled lithic clasts are andesitic to dacitic in composition. Little erosion had occurred at Láscar between the eruption in 1993 and our sampling during early 2006. We could therefore only sample the presently exposed surface of the deposits. Thermal demagnetization was performed on 124 samples cut from the clasts. Two main types of demagnetization behaviour are evident (Fig. 8). Most of the samples have a single magnetization component that is aligned with the 1993 geomagnetic field direction (Fig. 8a). An additional 18 samples, from dacitic clasts, provide evidence of self-reversing behaviour; the high temperature component is consistent with the 1993 geomagnetic field direction, but the lower temperature component is anti-parallel to this direction (Fig. 8b). The 1993 geomagnetic field direction is present up to the Curie temperature of these samples, which indicates that the clasts were fully remagnetized during the 1993 eruption.

Figure 9a is a stereoplot of the recorded paleomagnetic directions; the paleomagnetic directions are biased toward the 1993 geomagnetic field direction and its antipode. Figure 9b is a stereoplot of the recorded paleomagnetic directions that fall within 30° of the 1993 geomagnetic field direction; these clasts are used to estimate the emplacement temperature. Of

Fig. 7 **a** Location map of Láscar volcano along with a simplified geological map of the deposits from the 18–20 April, 1993, pyroclastic density currents. The geological map has been modified after Calder et al. (2000). **b** Thermal radiance map of the 1993 Láscar pyroclastic deposits modified after Denniss et al. (1998). The shape of the northern thermal anomaly mimics the shape of the pyroclastic deposits shown in (a). The eruption cloud obscured the pyroclastic deposits on the SE slope of Láscar, so no thermal radiance data are available for these deposits

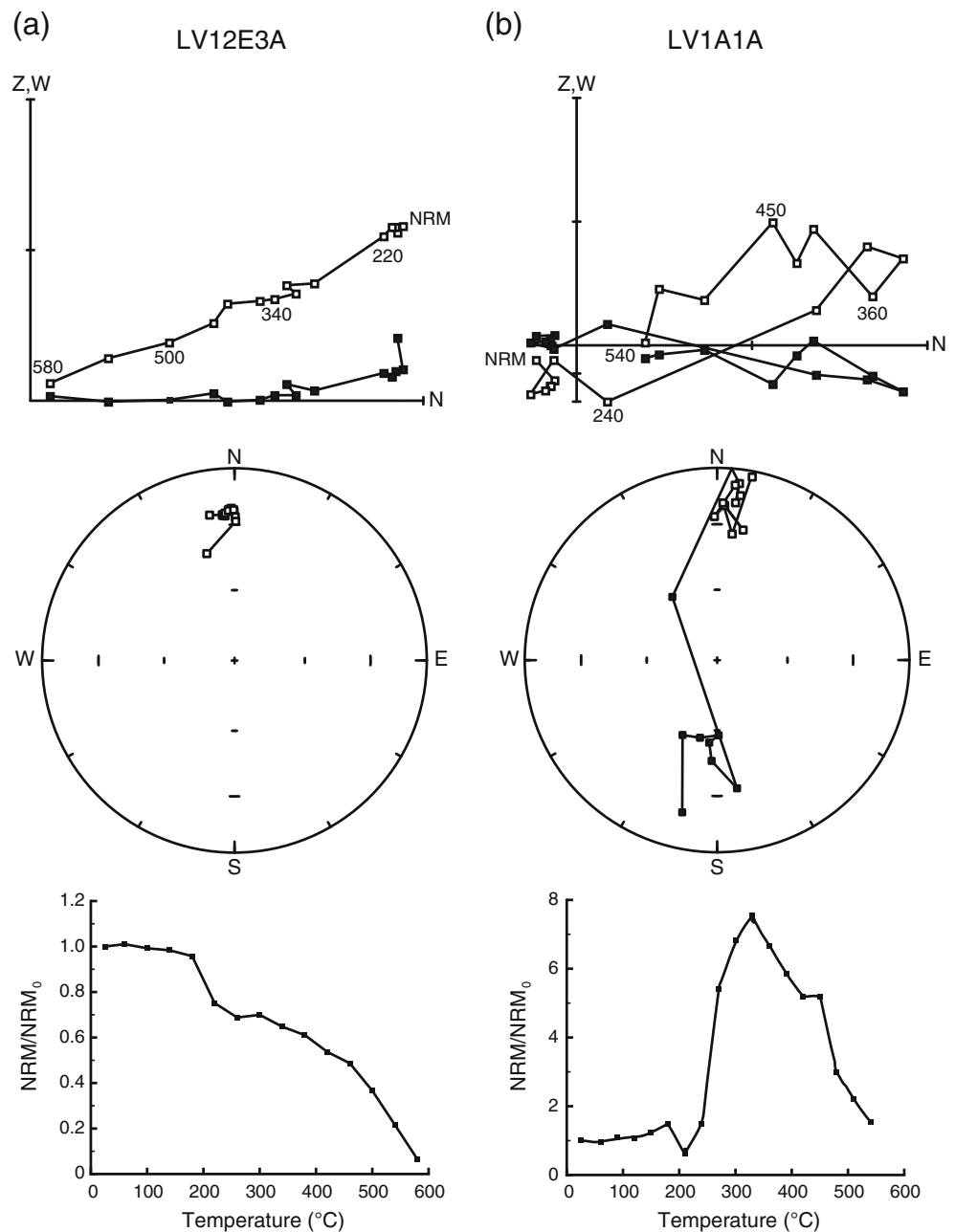


the samples with self-reversing magnetizations, 17 have well-defined normal and reverse polarity components of magnetization (with maximum angular deviation, $MAD \leq 15^\circ$; Kirschvink 1980). A further 11 samples have well-defined high temperature, normally magnetized components but have poorly defined ($MAD > 15^\circ$) low temperature components of magnetization, which fall close to the antipodal direction of the 1993 geomagnetic field. Due to their high MAD values, these low temperature components of magnetization are excluded from further analysis. A reversal test for the

two, well-defined directions (Fig. 9c) yields overlapping α_{95} cones of confidence, which indicates that the directions are antipodal. The reversal test of McFadden and McElhinny (1990) yields an angular separation, γ_0 , of 5.7° , and a critical angle, γ_c , of 6.5° . This constitutes a positive reversal test ($\gamma_0 < \gamma_c$) of quality classification 'B' ($5^\circ < \gamma_c \leq 10^\circ$).

A total of 80 samples (72 independent clasts) unambiguously recorded the Earth's magnetic field during the 1993 eruption, which includes samples from 30 of the 31 sites sampled. The paleomagnetic data for the

Fig. 8 Typical stepwise thermal demagnetization behaviour for the Láscaar samples. **a** Sample LV12E3A has a single component of magnetization that is aligned with the 1993 geomagnetic field direction. **b** Sample LV1A1A exhibits (noisy) self-reversing paleomagnetic behaviour, in which the high temperature component aligns with the expected geomagnetic direction and the low temperature component is anti-parallel to the expected direction. Symbols are the same as in Fig. 3



normal polarity component closely cluster around the ambient field direction during April 1993 (Fig. 9a, b). The paleomagnetic inclination is shallower by a few degrees; this inclination error is most likely caused by clast rotation during compaction of the deposits, as suggested by Hoblitt et al. (1985).

Each clast indicates emplacement temperatures in excess of T_c (Table 2, [Electronic supplementary material](#)). Thermomagnetic curves (Fig. 5c, d) yield T_c values from 397°C to 641°C, while T_c of the juvenile material ranges from 402°C to 599°C. Although there is

no lowest emplacement temperature on which to base an estimate of T_{dep} , the uniformly high temperature of both the juvenile material and the lithic clasts suggests a high T_{dep} value ($\geq 397^\circ\text{C}$).

Despite the consistently high emplacement temperatures at nearly all of the sampled sites, 9 samples yielded noisy data and failed to record the 1993 geomagnetic field direction. These samples were not included in any further analysis. Another 35 samples do not record consistent paleomagnetic directions. This normally indicates cold emplacement. At each site,

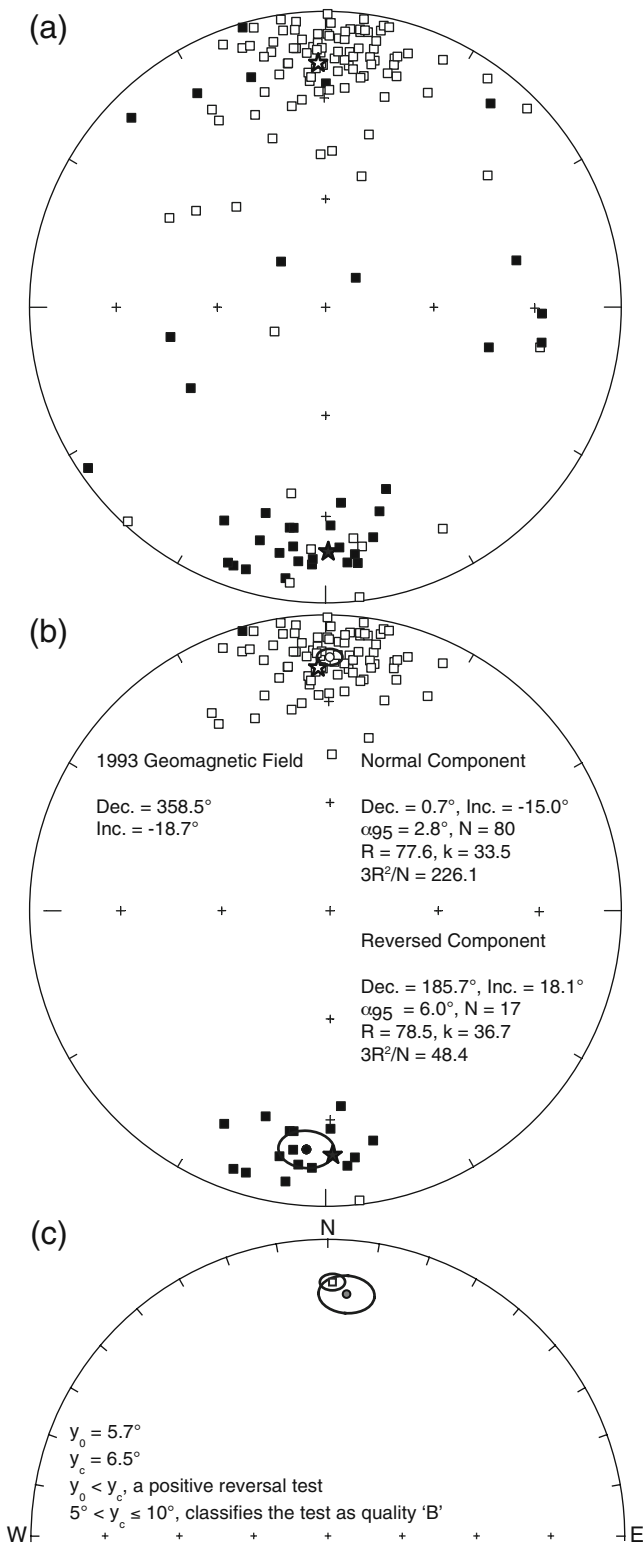


Fig. 9 Equal area stereographic projections of the paleomagnetic directions recorded by the samples collected at Láscar. The open star represents the direction of the Earth’s magnetic field during April 1993, and the filled star represents its antipode. **a** All of the recorded paleomagnetic directions. The distribution of directions is biased toward the direction of the 1993 geomagnetic field and its antipode (*solid star*). **b** The directions used for emplacement temperature estimation. The reversed polarity component represents data from 17 dacitic samples that exhibited self-reversing behaviour. *Symbols* are the same as in Fig. 4. **c** Reversal test for the mean paleomagnetic direction from the self-reversed samples compared to the mean direction for the normal polarity samples from Láscar. The *open square* represents the normally magnetized component and the *grey circle* represents the reversed polarity component with its declination rotated by 180°; the *ellipses* denote the respective α_{95} cones of 95% confidence. The overlapping confidence limits indicate that the directions are indistinguishable from a pair of antipodal directions. The reversal test of McFadden and McElhinny (1990) confirms this, and classifies the test as ‘B’ quality

emplaced cold and others hot. A much more likely scenario is that these samples have moved since they cooled. This interpretation is supported by the fact that only the surface of the deposit could be sampled.

Volcán de Colima, Mexico

The Colima Volcanic Complex, located in western Mexico, is a N-S trending volcanic chain consisting of three volcanoes: Volcán Cantaro, Nevado de Colima and Volcán de Colima (Fig. 10). Volcán de Colima is currently Mexico’s most active volcano with at least

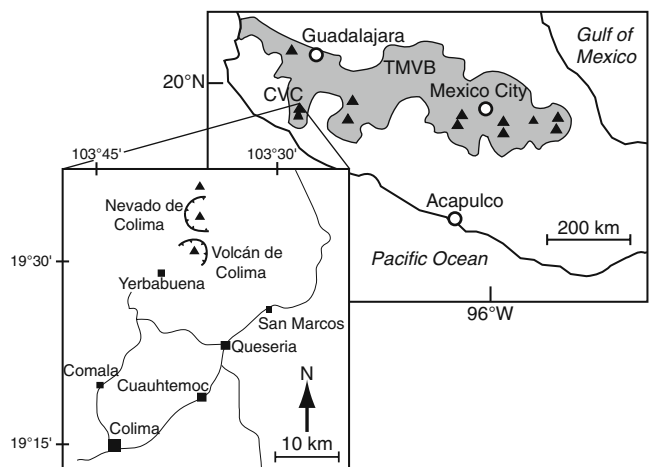


Fig. 10 Map of Central Mexico with the location of the Colima Volcanic Complex (CVC) within the Trans-Mexican Volcanic Belt (TMVB). The *inset* contains an expanded view of the CVC; the *lines* represent the main roads. Modified after Saucedo et al. (2002)

however, samples were collected from within a limited area and the distance between samples was typically less than 5 m. This suggests implausible temperature gradients within the deposit if some samples were

52 eruptions since 1560 A.D. (Bretón et al. 2002). Intermittent activity has been observed since 1998, with vulcanian eruptions, lava flows and growing domes that have collapsed and generated pyroclastic density currents (Saucedo et al. 2002; Zobin et al. 2002; Saucedo et al. 2004, 2005).

Thirteen localities were sampled from areas where pyroclastic eruptions occurred on June 2005 (VC1–7), January 1913 (VC8–11), and June 2004 (VC12–13). Two areas associated with the 2005 deposits were sampled where pyroclastic emplacement was observed, in the northern end of Montegrande gully (VC1–4), and further east in La Arena gully (VC5–7). Sites VC8–11 were located in the northern end of Zarco river valley, and samples from the 2004 deposits (VC12–13) were collected from the western flank of the volcano inside the Rio la Lumbre river valley. Thermal demagnetization was carried out on 133 samples from 107 clasts, which reveals both single and multiple magnetization components (Fig. 11a). A stereographic projection of all of the low temperature paleomagnetic components, which includes single remanence components, is shown in Fig. 11b. Only one of the paleomagnetic directions falls close to the geomagnetic field direction during the respective eruptions that produced the sampled deposits (indicated by the two stars). The test for randomness is not satisfied ($3R^2/N = 38.2$), which suggests a bias in the recorded directions toward a downward and southeastward direction, although no statistically reliable direction can be identified (Fig. 11b). The recorded paleomagnetic directions all have low MAD values, which indicates that the scatter of directions is not simply due to noise (Table 3, [Electronic supplementary material](#)). The lack of a contemporaneous geomagnetic field direction indicates that the sampled clasts were emplaced in their current deposits below the temperature at which the viscous overprint is removed, i.e., below $\sim 115^\circ\text{C}$ for the 2004/5 deposits and below $\sim 135^\circ\text{C}$ for the 1913 deposits. The wet local climate means that pyroclastic debris is frequently remobilized as lahars, often soon after an eruption (Davila et al. 2007). Therefore, the most probable explanation of the data distribution is that the sampled deposits represent reworked pyroclastics. The presence of numerous clasts with two components of magnetic remanence may suggest that the clasts have undergone reheating/remagnetization at some point in the past, which supports the hypothesis that the clasts are most likely sourced from pyroclastic deposits. The wide range of potential emplacement temperatures indicated by these multicomponent clasts (250–450°C)

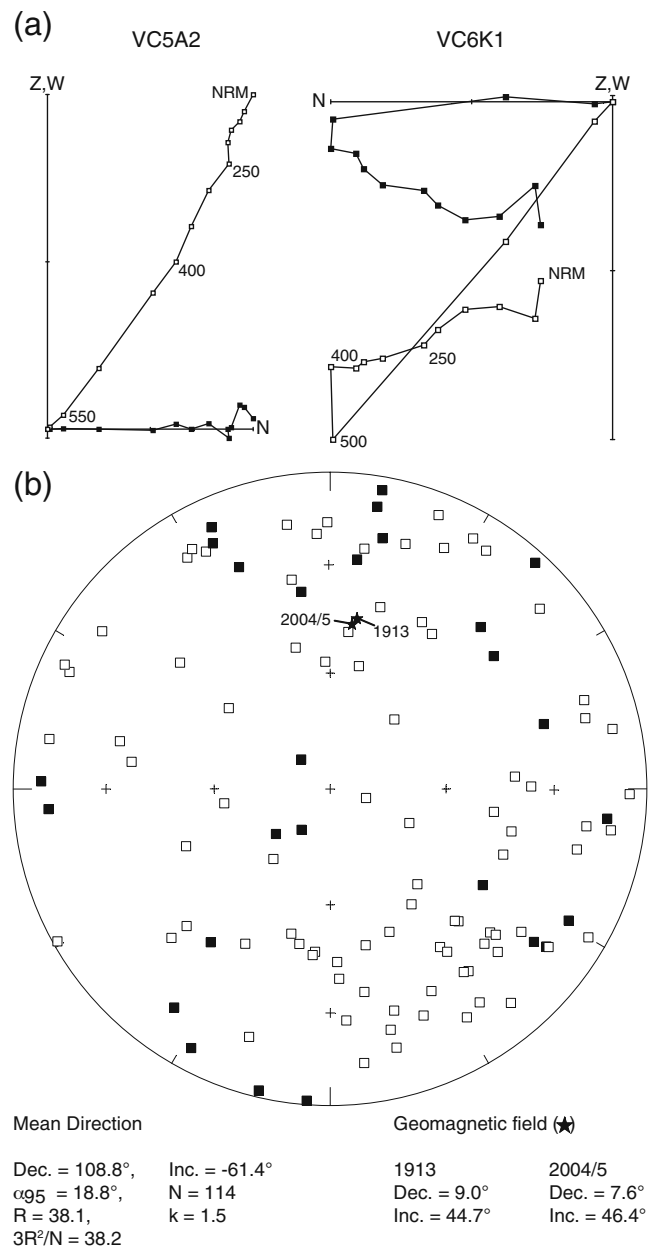


Fig. 11 **a** Vector component diagrams for samples VC5A2 and VC6K1, which represent examples of single and multiple component remanent magnetizations, respectively. Symbols are the same as in Fig. 3. **b** Equal area stereographic projection of the low temperature paleomagnetic directions recorded by the studied samples from Colima. The two stars represent the expected geomagnetic field directions from 1913, 2004/2005, which are nearly indistinct. There is no statistically identifiable direction from the measured paleomagnetic data, although there is a general bias toward a southeastward and upward direction. Symbols are the same as in Fig. 4

provides little information about the emplacement temperature of the reworked deposits because there is no constraint on the origin of the clasts (i.e., they

could be sourced from numerous deposits with varying emplacement temperature).

Numerous pieces of charred wood and plant debris are visible within the sampled deposits. The presence of these fragments suggests that the deposits were emplaced above ambient temperature, while the paleomagnetic evidence indicates that the deposits were emplaced at ambient temperature. The possibility of accessory materials being reworked into cold deposits and giving rise to false emplacement temperature estimates highlights the value of the paleomagnetic method for determining pyroclastic emplacement temperatures.

Vesuvius, Italy

Numerous investigations have been made of the temperature from the 79 A.D. eruption of Vesuvius using both paleomagnetic (e.g., Kent et al. 1981) and non-paleomagnetic methods (e.g., Mastrolorenzo et al. 2001). Kent et al. (1981), in their pioneering work on developing the paleomagnetic method, investigated lithic fragments and juvenile material from pyroclastic deposits in the town of Herculaneum. Their results suggest that the deposits could not have been hotter than $\sim 400^\circ\text{C}$. Both Capasso et al. (2000) and Mastrolorenzo et al. (2001) analysed bone fragments from the bodies of victims killed by the pyroclastics at Herculaneum. Capasso et al. (2000) estimated that the bones reached temperatures of up to $350\text{--}400^\circ\text{C}$, while Mastrolorenzo et al. (2001) suggested higher temperatures of $\sim 500^\circ\text{C}$. Mastrolorenzo et al. (2001) also used paleomagnetism to investigate a tile fragment, estimating its emplacement temperature to be 480°C . Cioni et al. (2004), using paleomagnetism, investigated the temperature of the pyroclastic deposits on a much wider scale, and sampled 13 sites around the volcano. Their results indicate that the pyroclastics were emplaced at temperatures of $180\text{--}380^\circ\text{C}$. Zanella et al. (2007) investigated the temperature of the 79 A.D. deposits at Pompeii in detail. These deposits reached temperatures up to 320°C , but were as cool as 180°C in some areas. This variation of a few hundred degrees over short distances illustrates the effect that urban areas can have on the temperature of pyroclastics and might explain the temperature variations documented at Herculaneum. Zanella et al. (2008) recently investigated the 472 A.D. deposits from Vesuvius. These deposits were uniformly hot with $T_{dep} \sim 260\text{--}360^\circ\text{C}$ irrespective of locality and the facies sampled. They concluded that the uniformity of deposit temperature can be attributed to similar rates of heat transfer from juvenile to lithic clasts and/or to similarity in deposition regimes of the different facies. Based on

the similar temperatures from both phreatomagmatic and magmatic facies, they also concluded that magma-water interactions had little influence on T_{dep} .

At our sampled locality, Pollena quarry (Fig. 12), Cioni et al. (2004) estimated the emplacement temperature of the 79 A.D. pyroclastics to be $250\text{--}310^\circ\text{C}$, while Zanella et al. (2008) estimated the 472 A.D. deposits to have been emplaced at $280\text{--}320^\circ\text{C}$. We sampled 124 lithic clasts from the 472 A.D. deposits at the Pollena quarry, on the western flank of Vesuvius (Fig. 12). Six sites were sampled from the lithic rich pyroclastic flow (LRPF) and the F_g facies described by Sulpizio et al. (2005, 2007). The sampled clasts are predominantly leucite-bearing tephrites, with occasional andesites and a syenite (Table 4, [Electronic supplementary material](#)). Any VRM should be removed by laboratory heating to $\sim 150^\circ\text{C}$, therefore data below this heating step are ignored.

Three main types of remanence behaviour are identified, with most samples having a single magnetization component (Fig. 13a). A number of samples have more complicated, multi-component magnetizations (Fig. 13b, c). Equal area stereographic projections of the low temperature magnetization components recorded at the six sampled sites are shown in Fig. 14. There is no consistency in the paleomagnetic directions at site CP1. Evidence of debris flows at this site raised doubts when sampling as to whether the site was *in-situ*; the paleomagnetic data confirm that these samples have been remobilized. At sites CP3–6 the paleomagnetic directions are biased toward a northward and downward direction. Only 3 samples were available from site CP2, but the same trend is still identifiable.

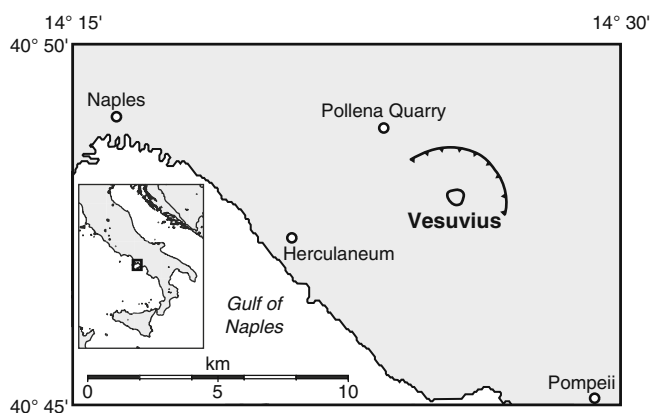


Fig. 12 Sketch map of the Vesuvius area, central Italy. All samples were collected from Pollena quarry on the north-western flank of Vesuvius

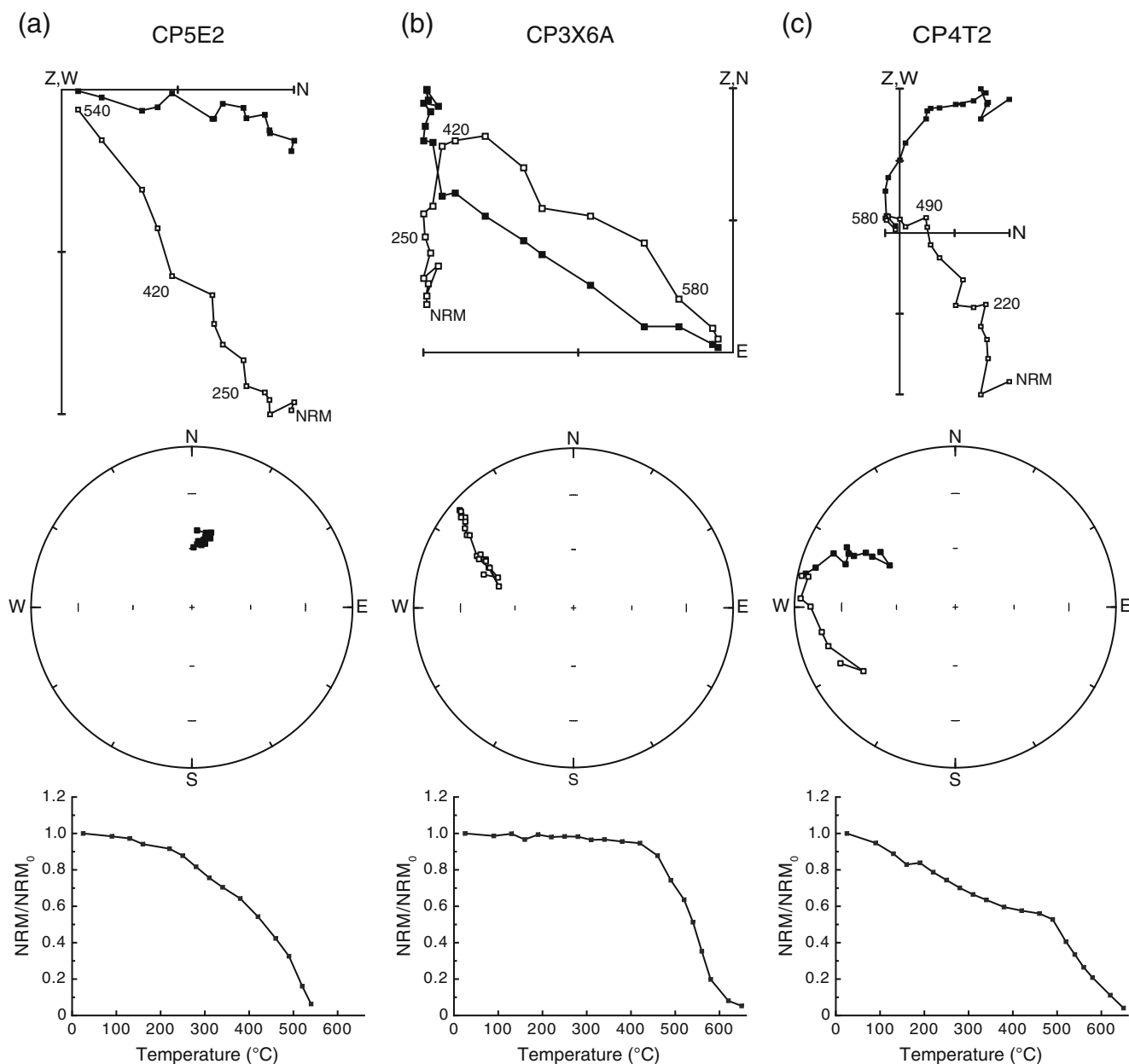


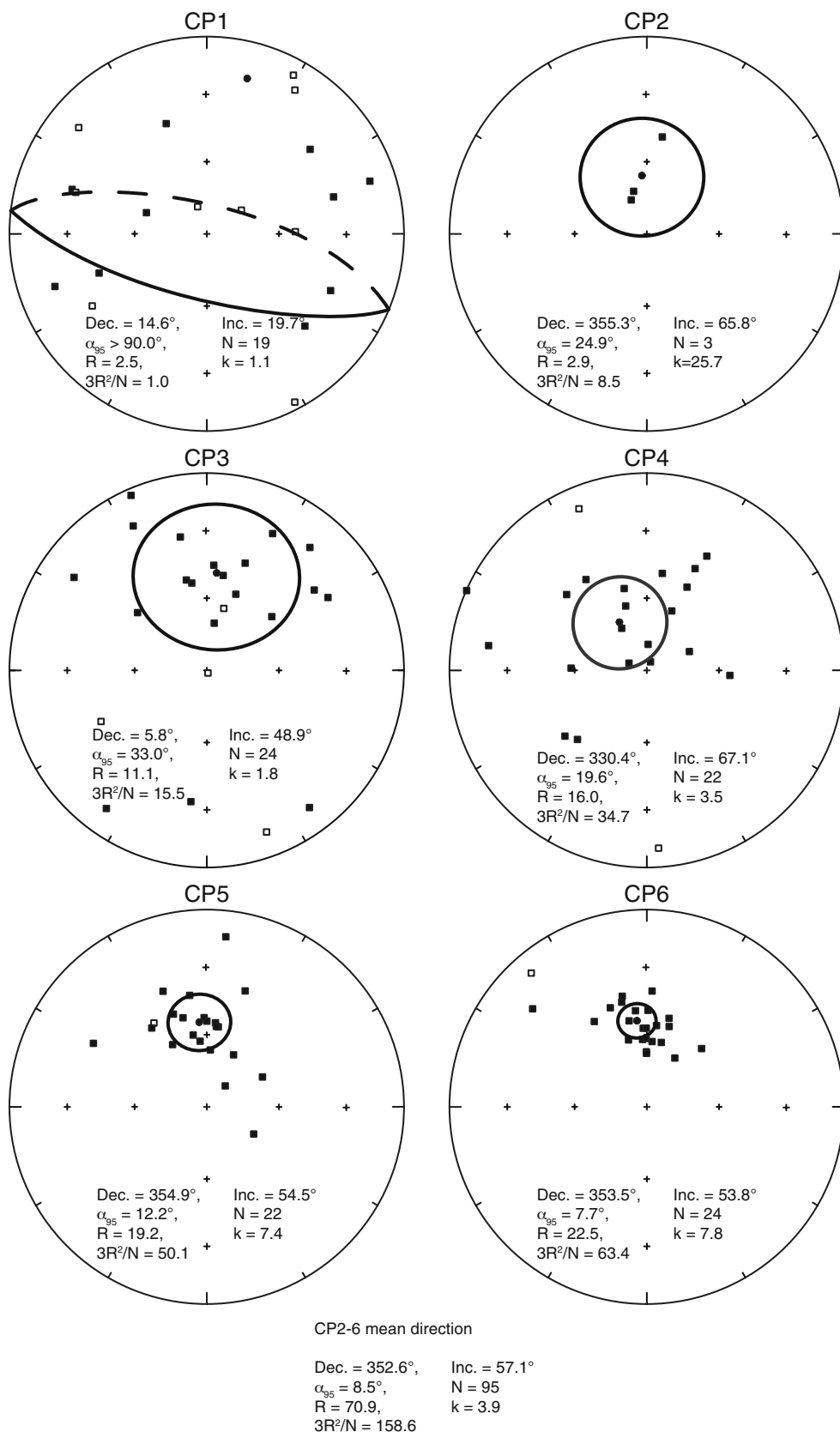
Fig. 13 Typical stepwise thermal demagnetization behaviour for the Vesuvius samples. **a** Sample CP5E2 has a single component of magnetization that coincides with the mean paleomagnetic direction recorded at sites CP2–6. **b** Sample CP3X6A has two components of magnetization, with the low temperature direc-

tion aligning with the mean direction at sites CP2–6. **c** Sample CP4T2 has three components of magnetization; the low temperature direction aligns with the expected mean direction, while neither higher temperature components have a preferred direction. Symbols are the same as in Fig. 3

At each of these sites, $3R^2/N$ exceeds 7.81 (Fig. 14), which indicates that the paleomagnetic directions are statistically grouped. A mean paleomagnetic direction was obtained by grouping sites CP2–6 (Dec. = 352.6° , Inc. = 57.1° , $\alpha_{95} = 8.5^\circ$, $N = 95$, $R = 70.9$, $k = 3.9$, $3R^2/N = 158.6$). This direction is consistent with paleomagnetic directions recorded in previous studies (e.g.,

Tanguy et al. 2003; Zanella et al. 2008)). To isolate clasts that record a consistent direction, data from sites CP2–6 were excluded if the paleomagnetic direction was $>30^\circ$ away from the mean paleomagnetic direction. Sixty-three clasts were thereby used to estimate emplacement temperatures. At least 3 clasts from each site met this selection criterion.

Fig. 14 Equal area stereographic projections of paleomagnetic directions recorded at each sample site at Vesuvius. Symbols are the same as in Fig. 4



Thermomagnetic analysis was carried out on all of these clasts (e.g., Fig. 5e, f). Sample CP4Q has a Curie temperature that coincides with its estimated emplacement temperature (Fig. 5e). This might be because the sample has a CRM, therefore it was excluded from further analysis. Sample CP6Q has behaviour that is typical of the inversion of maghemite to hematite and magnetite (Fig. 5f). This is strong evidence that maghemite is the main magnetic mineral and that the magnetic remanence of this lithic clast is a CRM. This sample was also removed from further consideration.

The three clasts from site CP2 (from the F_g facies) were remagnetized above the Curie temperature of their constituent magnetic minerals. T_c values range from 568 to 580°C (Table 4, [Electronic supplementary material](#)). The small number of samples precludes a reliable estimate of the deposit temperature at this locality. Sites CP3 and 4 are from the lower 2 m of the exposed LRPF within Pollena quarry. Variable emplacement temperatures were estimated from ~280°C to above T_c . The majority of clasts have multi-component remanences, which indicate emplacement between 310 and 460°C. The deposit temperature is constrained by the lowest temperature experienced by an individual clast. For site CP3, $T_{dep} = 310\text{--}340^\circ\text{C}$, and $T_{dep} = 280\text{--}340^\circ\text{C}$ for site CP4. T_{dep} of the lower section of the LRPF is 280–340°C. This agrees well with the estimate of Zanella et al. (2008) of $T_{dep} = 280\text{--}320^\circ\text{C}$. This result emphasizes the inter-laboratory repeatability of the paleomagnetic method. Sites CP5 and 6 are from the upper part of the LRPF. The majority of clasts from these sites were emplaced above T_c , but three clasts from site CP5 and two clasts from site CP6 were emplaced at ~520°C. Curie temperatures at these two sites range from 533 to 649°C. T_{dep} is taken to be ~520°C. This estimate is higher than the 280–320°C estimated by Zanella et al. (2008). The temperature contrast between the upper and lower LRPF and the data of Zanella et al. (2008) is large (~200°C). Few samples measured by Zanella et al. (2008) have single magnetization components that indicate full remagnetization of clasts (~1%); similarly, in this study the lower LRPF has relatively few fully remagnetized clasts. This suggests that the majority of clasts incorporated into this part of the deposit experienced little or no heating prior to deposition. In contrast, the upper section of the LRPF sampled in this study predominantly contains clasts that have been remagnetized above T_c . This suggests that these clasts have undergone considerable heating before deposition. From this we infer that the upper and lower sections of the LRPF have different sources of lithic clasts. The clasts from the lower LRPF are sourced from the cold debris on the flanks of the

volcano, while clasts from the upper LRPF are most likely to be vent-derived lithics that were initially hot.

Discussion

Determining the emplacement temperature of pyroclastic deposits can aid in the assessment of volcanic hazards. Establishing the thermal evolution of an eruptive phase or the entire thermal history of a volcano can help to refine predictions of hazards associated with future activity. Paleomagnetism provides an underutilized tool for such studies. We have used paleomagnetism to investigate the emplacement temperatures of pyroclastic deposits from historic eruptions of four volcanoes. Mt. St. Helens, USA, provides an ideal locality to test the paleomagnetic method against direct measurements taken shortly after deposition. Erwin (2001) highlighted the accuracy of the paleomagnetic method at Mt. St. Helens. We provide additional data, which further confirms the usefulness of the paleomagnetic method. Our analysis of clasts and juvenile material collected from the June and July 1980 pyroclastic deposits confirms the paleomagnetic determinations of Erwin (2001) and agrees well with the direct measurements of Banks and Hoblitt (1996). The three sampled localities of the June 1980 pyroclastics (MSH3, 5 and 6) were emplaced $\geq 532^\circ\text{C}$, $\geq 509^\circ\text{C}$ and at 510–570°C. For the July 1980 pyroclastics (MSH4), $T_{dep} \geq 577^\circ\text{C}$.

At Láscaar, Chile, paleomagnetic data also indicate that the clasts were emplaced above T_c at $\geq 397^\circ\text{C}$. Satellite imagery provides an estimate of $T_{dep} \geq 185\text{--}265^\circ\text{C}$ (Denniss et al. 1998). Satellite methods do not allow higher temperature estimates, so paleomagnetic determinations have proven more useful in this case. The presence, and inclusion, of samples that exhibit self-reversing behaviour may give rise to uncertainties with these estimates. Alternating field demagnetization data confirm that the NRM of the samples in question is affected by self-reversal, which indicates that the self-reversing mechanism occurred naturally and that it is not an artefact of thermal demagnetization. If we consider the directions recorded by the self-reversing and non-self-reversing samples independently, we can perform a statistical analysis to test if the two directions are distinguishable (e.g., Butler 1992). The F -statistic indicates that the two directions cannot be distinguished at the 95% confidence level, where $F = 0.332 \ll 3.054$ (the critical F value for the two datasets).

At Colima, Mexico, the opposite end of the spectrum is observed, where the sampled clasts were cold when emplaced into their current deposits. This suggests that the sampled deposits most likely represent lahars. This

illustrates the usefulness of paleomagnetism for discriminating between different types of deposits, which is useful when differentiation based on field or satellite observations is difficult.

Results from Vesuvius, Italy, highlight the potential of the paleomagnetic method to investigate the emplacement temperature of older deposits. Emplacement temperatures of the individual clasts range from $\sim 280^\circ\text{C}$ to above T_c ($\sim 533\text{--}649^\circ\text{C}$). The deposit temperature was $\sim 280\text{--}340^\circ\text{C}$ for sites CP3 and CP4 (lower section of the LRPF), and $\sim 520^\circ\text{C}$ for sites CP5 and CP6 (upper section of the LRPF). Few samples from sites CP5 and CP6 have two magnetization components, which suggests that the deposit was emplaced close to T_c . We attribute the higher emplacement temperature recorded from the lower LRPF compared to the upper LRPF to changes in the source of lithic material. The lower LRPF contains initially cold lithic clasts, while the upper section contains initially hot clasts that were most likely sourced from or close to the volcanic vent.

Conclusions

This study highlights a number of key advantages in using the paleomagnetic method to determine the emplacement temperature of pyroclastic deposits.

1. The paleomagnetic method is as accurate as directly measuring temperatures shortly after deposition. Paleomagnetic sampling has the added benefit of not having to visit an active volcanic region immediately after an eruption.
2. The method is repeatable between laboratories, which allows reliable comparisons between different measurements.
3. Paleomagnetism provides a wide temperature range for estimating emplacement temperatures, up to $580\text{--}675^\circ\text{C}$, depending on the magnetic minerals present.
4. The method has a much wider emplacement temperature range than can be determined from satellite data and can be applied in the absence of materials such as wood or man-made materials, which may not always be present.
5. The presence of charred materials in reworked deposits provides ambiguity that can be resolved with paleomagnetism, which highlights the possibility that such proxies may give inaccurate emplacement temperature estimates.
6. The paleomagnetic method can be used to investigate emplacement temperatures over long time

scales. Stable recordings of the geomagnetic field can be carried by single domain magnetic grains over billions of years. This contrasts with direct measurements that are limited to recent and future events. Man-made materials are only available over the past several thousand years, and useful charred wood fragments are unlikely to survive over long time scales.

Acknowledgements This study was funded by NERC grant NER/S/A/2005/13478. Collection of the Mt. St. Helens, Colima and Vesuvius samples was funded through a Royal Society grant to ARM. We thank Karen Paola Guzmán Montenegro for assistance with collecting samples from Láscar, Jose Guadalupe Landin Orozco for assisting with sampling at Colima and Francesca Lawley and Andrew Harris for assistance at Vesuvius. We thank Michelle Harris for assistance with lithology classification. We also thank two anonymous reviewers for their helpful comments that improved the manuscript.

References

- Alva-Valdivia LM, Rosas-Elguera J, Bravo-Medina T, Urrutia-Fucugauchi J, Henry B, Caballero C, Rivas-Sanchez ML, Goguitchaichvili A, Lopez-Loera H (2005) Paleomagnetic and magnetic fabric studies of the San Gaspar ignimbrite, western Mexico—constraints on emplacement mode and source vents. *J Volcanol Geotherm Res* 147:68–80. doi:10.1016/j.jvolgeores.2005.03.006
- Aramaki S, Akimoto S (1957) Temperature estimation of pyroclastic deposits by natural remanent magnetism. *Am J Sci* 255:619–627
- Banks NG, Hoblitt R (1981) Summary of temperature studies of 1980 deposits. In: Lipman PW, Mullineaux DR (eds) *The 1980 eruptions of Mount St. Helens, Washington*. US Geol Surv Prof Pap 1250:295–313
- Banks NG, Hoblitt RP (1996) Direct temperature measurements of deposits, Mount St. Helens, Washington, 1980–1981. *US Geol Surv Prof Pap* 1387:1–76
- Bardot L (2000) Emplacement temperature determinations of proximal pyroclastic deposits on Santorini, Greece, and their implications. *Bull Volcanol* 61:450–467. doi:10.1007/PL00008911
- Bardot L, McClelland E (2000) The reliability of emplacement temperature estimates using palaeomagnetic methods: a case study from Santorini, Greece. *Geophys J Int* 143:39–51. doi:10.1046/j.1365-246x.2000.00186.x
- Bardot L, Thomas R, McClelland E (1996) Emplacement temperatures of pyroclastic deposits on Santorini deduced from palaeomagnetic measurements: constraints on eruption mechanisms. In: Morris A, Tarling DH (eds) *Palaeomagnetism and tectonics of the Mediterranean region*. Geol Soc London Spec Pub 105:345–357
- Bol'shakov, AS, Shcherbakova VV (1979) Thermomagnetic criterion for determining the domain structure of ferrimagnetics. *Izv Acad Sci USSR Phys Solid Earth* 15:111–117
- Bretón M, Ramírez JJ, Navarro C (2002) Summary of the historical eruptive activity of Volcán De Colima, Mexico 1519–2000. *J Volcanol Geotherm Res* 117:21–46. doi:10.1016/S0377-0273(02)00233-0

- Butler, RF (1992). *Paleomagnetism: magnetic domains to geologic terranes*. Blackwell Scientific, Boston
- Calder ES, Cole PD, Dade WB, Druitt TH, Hoblitt RP, Huppert HE, Ritchie L, Sparks RSJ, Young SR (1999) Mobility of pyroclastic flows and surges at the Soufrière Hills Volcano, Montserrat. *Geophys Res Lett* 26:537–540. doi:10.1029/1999GL900051
- Calder ES, Sparks RSJ, Gardeweg MC (2000) Erosion, transport and segregation of pumice and lithic clasts in pyroclastic flows inferred from ignimbrite at Láscar Volcano, Chile. *J Volcanol Geotherm Res* 104:201–235. doi:10.1016/S0377-0273(00)00207-9
- Capasso L, Caramiello S, D'Anastasio R, Di Domenicantonio L, Di Fabrizio A, Di Nardo F, La Verghetta M (2000) Paleobiologia della popolazione di Ercolano (79 dC). *Recenti Prog Med* 91:288–296
- Chadwick RA (1971) Paleomagnetic criteria for volcanic breccia emplacement. *Geol Soc Amer Bull* 82:2285–2294. doi:10.1130/0016-7606(1971)82[2285:PCFVBE]2.0.CO;2
- Cioni R, Gurioli L, Lanza R, Zanella E (2004) Temperatures of the AD 79 pyroclastic density current deposits (Vesuvius, Italy). *J Geophys Res* 109:B02207. doi:10.1029/2002JB002251
- Clement BM, Conner CB, Graper G (1993) Paleomagnetic estimate of the emplacement temperature of the long-runout Nevado De Colima Volcanic debris avalanche deposit, Mexico. *Earth Planet Sci Lett* 120:499–510
- Cole PD, Calder ES, Druitt TH, Hoblitt R, Robertson R, Sparks RSJ, Young SR (1998) Pyroclastic flows generated by gravitational instability of the 1996–97 lava dome of Soufrière Hills Volcano, Montserrat. *Geophys Res Lett* 25:3425–3428. doi:10.1029/98gl01510
- Crandell D (1971) Postglacial lahars from Mount Rainier Volcano, Washington. *US Geol Surv Prof Pap* 677:1–75
- Crandell DR, Mullineaux DR (1973) Pine creek volcanic assemblage at Mount St. Helens, Washington. *US Geol Surv Bull* 1383-A:1–23
- Davila N, Capra L, Gavilanes-Ruiz JC, Varley N, Norini G, Vazquez AG (2007) Recent lahars at Volcán de Colima (Mexico): drainage variation and spectral classification. *J Volcanol Geotherm Res* 165:127–141. doi:10.1016/j.jvolgeores.2007.05.016
- De Gennaro M, Naimo D, Gialenella P, Incoronato A, Mastrolorenzo G (1996) Palaeomagnetic controls on the emplacement of the Neapolitan Yellow Tuff (Campi Flegrei, Southern Italy). In: Morris A, Tarling DH (eds) *Palaeomagnetism and tectonics of the Mediterranean region*. *Geol Soc London Spec Pub* 105:359–365
- Denniss AM, Carlton RWT, Harris AJL, Rothery DA, Francis PW (1998) Satellite observations of the April 1993 eruption of Láscar Volcano. *Int J Remote Sens* 19:801–821. doi:10.1080/014311698215739
- Déruelle B, Medina ET, Figueroa OA, Maragano MC, Viramonté JG (1995) The recent eruption of Láscar volcano (Atacama-Chile, April 1993): petrological and volcanological relationships. *C R Acad Sci Paris* 321:377–384
- Déruelle B, Figueroa OA, Medina ET, Viramonté JG, Maragano MC (1996) Petrology of pumices of April 1993 eruption of Láscar (Atacama, Chile). *Terra Nova* 8:191–199. doi:10.1111/j.1365-3121.1996.tb00744.x
- Di Vito MA, Zanella E, Gurioli L, Lanza R, Sulpizio R, Bishop J, Tema E, Boenzi G, Laforgia E (2009) The Afragola settlement near Vesuvius, Italy: the destruction and abandonment of a bronze age village revealed by archaeology, volcanology and rock-magnetism. *Earth Planet Sci Lett* 277:408–421. doi:10.1016/j.epsl.2008.11.006
- Downey WS, Tarling DH (1991) Reworking characteristics of Quaternary pyroclastics, Thera (Greece), determined using magnetic properties. *J Volcanol Geotherm Res* 46:143–155. doi:10.1016/0377-0273(91)90080-J
- Druitt TH, Calder ES, Cole PD, Hoblitt RP, Loughlin SC, Norton GE, Ritchie LJ, Sparks RSJ, Voight B (2002) Small-volume, highly mobile pyroclastic flows formed by rapid sedimentation from pyroclastic surges at Soufriere Hills Volcano, Montserrat; an important volcanic hazard. In: Druitt DH, Kokelaar B (eds) *The eruption of Soufrière Hills Volcano, Montserrat, from 1995 to 1999*. *Mem Geol Soc Lond* 21:263–279
- Dunlop DJ (1971) Magnetic properties of fine-particle hematite. *Ann Geophys* 27:269–293
- Erwin PS (2001) *Palaeomagnetic investigations of volcano instability*. PhD thesis, University of Oxford, Oxford
- Fabian, K (2003) Statistical theory of weak field thermoremanent magnetization in multidomain particle ensembles. *Geophys J Int* 155:479–488. doi:10.1046/j.1365-246X.2003.02057.x
- Fisher RA (1953) Dispersion on a sphere. *Proc R Soc Lond A* 217:295–305. doi:10.1098/rspa.1953.0064
- Grubensky MJ, Smith GA, Geissman JW (1998) Field and paleomagnetic characterization of lithic and scoriaceous breccias at Pleistocene Broken Top volcano, Oregon Cascades. *J Volcanol Geotherm Res* 83:93–114. doi:10.1016/S0377-0273(98)00006-7
- Hoblitt RP, Kellogg KS (1979) Emplacement temperatures of unsorted and unstratified deposits of volcanic rock debris as determined by paleomagnetic techniques. *Geol Soc Amer Bull* 90:633–642
- Hoblitt RP, Reynolds RL, Larson EE (1985) Suitability of non-welded pyroclastic-flow deposits for studies of magnetic secular variation: a test based on deposits emplaced at Mount St. Helens, Washington, in 1980. *Geology* 13:242–245. doi:10.1130/0091-7613(1985)13<242:SONPDF>2.0.CO;2
- Kent DV, Ninkovitch D, Pescatore T, Sparks RSJ (1981) Palaeomagnetic determination of emplacement temperature of the Vesuvius AD 79 pyroclastic deposits. *Nature* 290:393–396. doi:10.1038/290393a0
- Kirschvink JL (1980) The least-squares line and plane and the analysis of palaeomagnetic data. *Geophys J R Astron Soc* 62:699–718
- Leonhardt R (2006) Analyzing rock magnetic measurements: the RockMagAnalyzer 1.0 software. *Comput Geosci* 32:1420–1431
- Levi, S (1977) Effect of magnetite particle-size on paleointensity determinations of geomagnetic-field. *Phys Earth Planet Inter* 13:245–259. doi:10.1016/0031-9201(77)90107-8
- Mandeville C, Carey S, Sigurdsson H, King J (1994) Paleomagnetic evidence for high-temperature emplacement of the 1883 subaqueous pyroclastic flows from Krakatau Volcano, Indonesia. *J Geophys Res* 99:9487–9504. doi:10.1029/94jb00239
- Mastrolorenzo G, Petrone PP, Pagano M, Incoronato A, Baxter PJ, Canzanella A, Fattore L (2001) Herculaneum victims of Vesuvius in AD 79. *Nature* 410:769–770. doi:10.1038/35071167
- Maury R (1971) Application de la spectrometrie infra-rouge a l'etude des bois fossilises dans les formations volcaniques. *Bull Soc Geol Fr* 5:280
- McClelland E, Druitt DH (1989) Palaeomagnetic estimates of emplacement temperatures of pyroclastic deposits on Santorini, Greece. *Bull Volcanol* 51:16–27. doi:10.1007/BF01086758
- McClelland E, Erwin PS (2003) Was a dacite dome implicated in the 9,500 BP collapse of Mt Ruapehu? A

- palaeomagnetic investigation. *Bull Volcanol* 65:294–305. doi:[10.1007/s00445-002-0261-y](https://doi.org/10.1007/s00445-002-0261-y)
- McClelland E, Thomas R (1993) A palaeomagnetic study of Minoan age tephra from Thera. In: Hardy D (ed) *Thera and the Aegean world III*, vol 2. Thera Foundation, London, pp 129–138
- McClelland E, Wilson CJN, Bardot L (2004) Palaeotemperature determinations for the 1.8-ka Taupo ignimbrite, New Zealand, and implications for the emplacement history of a high-velocity pyroclastic flow. *Bull Volcanol* 66:492–513. doi:[10.1007/s00445-003-0335-5](https://doi.org/10.1007/s00445-003-0335-5)
- McFadden PL, McElhinny MW (1990) Classification of the reversal test in palaeomagnetism. *Geophys J Int* 103:725–729. doi:[10.1111/j.1365-246X.1990.tb05683.x](https://doi.org/10.1111/j.1365-246X.1990.tb05683.x)
- Moore JD, Geissman JW, Smith GA (1997) Paleomagnetic emplacement-temperature and thermal-profile estimates for nonwelded pyroclastic-flow deposits, Miocene Peralta Tuff, Jemez Mountains, New Mexico. *EOS Trans AGU* 78:178
- Mullineaux DR, Crandell DR (1962) Recent lahars from Mount St. Helens, Washington. *Geol Soc Amer Bull* 73:855–870
- Néel L (1949) Théorie du traînage magnétique des ferromagnétiques en grains fins avec applications aux terres cuites. *Ann Geophys* 5:99–136
- Oppenheimer C, Glaze LS, Francis PW, Rothery DA, Carlton RWT (1993) Infrared image analysis of volcanic thermal features: Lascar Volcano, Chile, 1984–1992. *J Geophys Res* 98:4269–4286. doi:[10.1029/92jb02134](https://doi.org/10.1029/92jb02134)
- Pares JM, Marti J, Garces M (1993) Thermoremanence in red sandstone clasts and emplacement temperature of a Quaternary pyroclastic deposit (Catalan Volcanic Zone, NE Spain). *Stud Geophys Geod* 37:401–414
- Petrovský E, Kapička A (2006) On determination of the Curie point from thermomagnetic curves. *J Geophys Res* 111:B12S27. doi:[10.1029/2006JB004507](https://doi.org/10.1029/2006JB004507)
- Porreca M, Giordano G, Mattei M, Musacchio P (2006) Evidence of two Holocene phreatomagmatic eruptions at Stromboli volcano (Aeolian Islands) from paleomagnetic data. *Geophys Res Lett* 33:L21316. doi:[10.1029/2006GL027575](https://doi.org/10.1029/2006GL027575)
- Porreca M, Mattei M, Mac Niocaill C, Giordano G, McClelland E, Funicello R (2007) Paleomagnetic evidence for low-temperature emplacement of the phreatomagmatic Peperino Albano ignimbrite (Colli Albani volcano, Central Italy). *Bull Volcanol* 70:877–893. doi:[10.1007/s00445-007-0176-8](https://doi.org/10.1007/s00445-007-0176-8)
- Pullaiah G, Irving E, Buchan KL, Dunlop DJ (1975) Magnetization changes caused by burial and uplift. *Earth Planet Sci Lett* 28:133–143. doi:[10.1016/0012-821X\(75\)90221-6](https://doi.org/10.1016/0012-821X(75)90221-6)
- Rayleigh L (1919) On a problem of vibrations, and of random flights in one, two and three dimensions. *Phila Mag* 37:321–347
- Saito T, Ishikawa N, Kamata H (2003) Identification of magnetic minerals carrying NRM in pyroclastic-flow deposits. *J Volcanol Geotherm Res* 126:127–142. doi:[10.1016/S0377-0273\(03\)00132-X](https://doi.org/10.1016/S0377-0273(03)00132-X)
- Saucedo R, Macías JL, Bursik MI, Mora JC, Gavilanes JC, Cortes A (2002) Emplacement of pyroclastic flows during the 1998–1999 eruption of Volcán de Colima, Mexico. *J Volcanol Geotherm Res* 117:129–153. doi:[10.1016/S0377-0273\(02\)00241-X](https://doi.org/10.1016/S0377-0273(02)00241-X)
- Saucedo R, Macías JL, Bursik MI (2004) Pyroclastic flow deposits of the 1991 eruption of Volcán de Colima, Mexico. *Bull Volcanol* 66:291–306. doi:[10.1007/s00445-003-0311-0](https://doi.org/10.1007/s00445-003-0311-0)
- Saucedo R, Macías JL, Sheridan MF, Bursik MI, Komorowski JC (2005) Modeling of pyroclastic flows of Colima Volcano, Mexico: implications for hazard assessment. *J Volcanol Geotherm Res* 139:103–115. doi:[10.1016/j.jvolgeores.2004.06.019](https://doi.org/10.1016/j.jvolgeores.2004.06.019)
- Sawada Y, Sampei Y, Hyodo M, Yagami T, Fukue M (2000) Estimation of emplacement temperatures of pyroclastic flows using H/C ratios of carbonized wood. *J Volcanol Geotherm Res* 104:1–20. doi:[10.1016/S0377-0273\(00\)00196-7](https://doi.org/10.1016/S0377-0273(00)00196-7)
- Shcherbakova VV, Shcherbakov VP, Heider F (2000) Properties of partial thermoremanent magnetization in pseudosingle domain and multidomain magnetite grains. *J Geophys Res* 105:767–781. doi:[10.1029/1999JB900235](https://doi.org/10.1029/1999JB900235)
- Smith GA, Grubensky MJ, Geissman JW (1999) Nature and origin of cone-forming volcanic breccias in the Te Herenga Formation, Ruapehu, New Zealand. *Bull Volcanol* 61:64–82. doi:[10.1007/s004450050263](https://doi.org/10.1007/s004450050263)
- Smithsonian Institution (1980) Mount St. Helens. Scientific Event Alert Network (SEAN) Bulletin 5
- Smithsonian Institution (1993) Lascar. Scientific Event Alert Network (SEAN) Bulletin 18
- Sparks RSJ, Gardeweg MC, Calder ES, Matthews SJ (1997) Erosion by pyroclastic flows on Lascar volcano Chile. *Bull Volcanol* 58:557–565. doi:[10.1007/s004450050162](https://doi.org/10.1007/s004450050162)
- Sulpizio R, Mele D, Dellino P, La Volpe L (2005) A complex, Subplinian-type eruption from low-viscosity, phonolitic to tephri-phonolitic magma: the AD 472 (Pollena) eruption of Somma-Vesuvius, Italy. *Bull Volcanol* 67:743–767. doi:[10.1007/s00445-005-0414-x](https://doi.org/10.1007/s00445-005-0414-x)
- Sulpizio R, Mele D, Dellino P, La Volpe L (2007) Deposits and physical properties of pyroclastic density currents during complex Subplinian eruptions: the AD 472 (Pollena) eruption of Somma-Vesuvius, Italy. *Sedimentology* 54:607–635. doi:[10.1111/j.1365-3091.2006.00852.x](https://doi.org/10.1111/j.1365-3091.2006.00852.x)
- Sulpizio R, Zanella E, Macías JL (2008) Deposition temperature of some PDC deposits from the 1982 eruption of El Chichón volcano (Chiapas, Mexico) inferred from rock-magnetic data. *J Volcanol Geotherm Res* 175:494–500. doi:[10.1016/j.jvolgeores.2008.02.024](https://doi.org/10.1016/j.jvolgeores.2008.02.024)
- Tamura Y, Koyama M, Fiske RS (1991) Paleomagnetic evidence for hot pyroclastic debris flow in the shallow submarine Shirahama Group (Upper Miocene-Pliocene) Japan. *J Geophys Res* 96:21779–21787. doi:[10.1029/91jb02258](https://doi.org/10.1029/91jb02258)
- Tanaka H, Hoshizumi H, Iwasaki Y, Shibuya H (2004) Applications of paleomagnetism in the volcanic field: a case study of the Unzen Volcano, Japan. *Earth Planets Space* 56:635–647
- Tanguy J-C, Le Goff M, Principe C, Arrighi S, Chillemi V, Paiotti A, La Delfa S, Patanè G (2003) Archeomagnetic dating of Mediterranean volcanics of the last 2100 years: validity and limits. *Earth Planet Sci Lett* 211:111–124. doi:[10.1016/S0012-821X\(03\)00186-9](https://doi.org/10.1016/S0012-821X(03)00186-9)
- Tanguy J-C, Ribiere C, Scarth A, Tjetjep WS (1998) Victims from volcanic eruptions: a revised database. *Bull Volcanol* 60:137–144. doi:[10.1007/s004450050222](https://doi.org/10.1007/s004450050222)
- Tarling DH (1983) *Palaeomagnetism: principles and applications in geology, geophysics and archaeology*. Chapman and Hall, London
- Tsuboi S, Tsuya H (1930) On the temperature of the pumiceous ejecta of Komagatake, Hokkaidō, as inferred from their modes of oxidation. *Bull Earthq Res Inst Univ Tokyo* 8:271–273
- Voight B, Davis MJ (2000) Emplacement temperatures of the November 22, 1994 nuée ardente deposits, Merapi Volcano, Java. *J Volcanol Geotherm Res* 100:371–377. doi:[10.1016/S0377-0273\(00\)00146-3](https://doi.org/10.1016/S0377-0273(00)00146-3)
- Witham CS (2005) Volcanic disasters and incidents: a new database. *J Volcanol Geotherm Res* 148:191–233. doi:[10.1016/j.jvolgeores.2005.04.017](https://doi.org/10.1016/j.jvolgeores.2005.04.017)

- Wooster MJ (2001) Long-term infrared surveillance of Láscar Volcano: contrasting activity cycles and cooling pyroclastics. *Geophys Res Lett* 28:847–850. doi:[10.1029/2000gl011904](https://doi.org/10.1029/2000gl011904)
- Wooster MJ, Rothery DA (1997) Thermal monitoring of Láscar volcano, Chile, using infrared data from the along-track scanning radiometer: a 1992–1995 time series. *Bull Volcanol* 58:566–579. doi:[10.1007/s004450050163](https://doi.org/10.1007/s004450050163)
- Wooster MJ, Carlton RWT, Rothery DA, Sear CB (1998) Monitoring the development of active lava domes using data from the ERS-1 along track scanning radiometer. *Adv Space Res* 21:501–505. doi:[10.1016/S0273-1177\(97\)00887-9](https://doi.org/10.1016/S0273-1177(97)00887-9)
- Wright J (1978) Remanent magnetism of poorly sorted deposits from the Minoan eruption of Santorini. *Bull Volcanol* 41:131–135. doi:[10.1007/BF02597026](https://doi.org/10.1007/BF02597026)
- Xu WX, Peacor DR, VanderVoo R, Dollase W, Beaubouef R (1996) Modified lattice parameter Curie temperature diagrams for titanomagnetite/titanomaghemite within the quadrilateral $\text{Fe}_3\text{O}_4\text{--Fe}_2\text{TiO}_4\text{--Fe}_2\text{O}_3\text{--Fe}_2\text{TiO}_5$. *Geophys Res Lett* 23:2811–2814. doi:[10.1029/96GL01117](https://doi.org/10.1029/96GL01117)
- Yamazaki T, Kato I, Muroi I, Abe M (1973) Textural analysis and flow mechanism of the Donzurubo subaqueous pyroclastic flow deposits. *Bull Volcanol* 37:231–244. doi:[10.1007/BF02597132](https://doi.org/10.1007/BF02597132)
- Zanella E, De Astis G, Lanza R (2001) Palaeomagnetism of welded, pyroclastic-fall scoriae at Vulcano, Aeolian Archipelago. *J Volcanol Geotherm Res* 107:71–86. doi:[10.1016/S0377-0273\(00\)00298-5](https://doi.org/10.1016/S0377-0273(00)00298-5)
- Zanella E, Gurioli L, Pareschi MT, Lanza R (2007) Influences of urban fabric on pyroclastic density currents at Pompeii (Italy): 2. Temperature of the deposits and hazard implications. *J Geophys Res* 112:B05214. doi:[10.1029/2006JB004775](https://doi.org/10.1029/2006JB004775)
- Zanella E, Gurioli L, Lanza R, Sulpizio R, Bontempi M (2008) Deposition temperature of the AD 472 Pollena pyroclastic density current deposits, Somma-Vesuvius, Italy. *Bull Volcanol* 70:1237–1248. doi:[10.1007/s00445-008-0199-9](https://doi.org/10.1007/s00445-008-0199-9)
- Zijderveld JDA (1967) AC demagnetization of rocks: analysis of results. In: Collinson DW, Creer KM, Runcorn SK (eds) *Methods in palaeomagnetism*. Elsevier, New York, pp 256–286
- Zlotnicki J, Pozzi JP, Boudon G, Moreau MG (1984) A new method for the determination of the setting temperature of pyroclastic deposits (example of Guadeloupe–French-West-Indies). *J Volcanol Geotherm Res* 21:297–312. doi:[10.1016/0377-0273\(84\)90027-1](https://doi.org/10.1016/0377-0273(84)90027-1)
- Zobin VM, Luhr JF, Taran YA, Bretón M, Cortés A, De La Cruz-Reyna S, Domínguez T, Galindo I, Gavilanes JC, Muñíz JJ, Navarro C, Ramírez JJ, Reyes GA, Ursúa M, Velasco J, Alatorre E, Santiago H (2002) Overview of the 1997–2000 activity of Volcán de Colima, México. *J Volcanol Geotherm Res* 117:1–19. doi:[10.1016/S0377-0273\(02\)00232-9](https://doi.org/10.1016/S0377-0273(02)00232-9)